

Induced Ginibre ensemble of random matrices and quantum operations

Jonit Fischmann¹, Wojciech Bruzda², Boris A Khoruzhenko¹,
Hans-Jürgen Sommers³ and Karol Życzkowski^{2,4}

¹ Queen Mary University of London, School of Mathematical Sciences, London E1 4NS, UK

² Institute of Physics, Jagiellonian University, ul. Reymonta 4, 30-059 Kraków, Poland

³ Fakultät Physik, Universität Duisburg-Essen, 47048 Duisburg, Germany

⁴ Center for Theoretical Physics, Polish Academy of Sciences, Al. Lotników 32/44,
02-668 Warszawa, Poland

E-mail: j.fischmann@qmul.ac.uk, w.bruzda@uj.edu.pl, b.khoruzhenko@qmul.ac.uk,
h.j.sommers@uni-due.de and karol@tatry.if.uj.edu.pl

Received 16 August 2011, in final form 28 December 2011

Published 1 February 2012

Online at stacks.iop.org/JPhysA/45/075203

Abstract

A generalization of the Ginibre ensemble of non-Hermitian random square matrices is introduced. The corresponding probability measure is induced by the ensemble of rectangular Gaussian matrices via a quadratization procedure. We derive the joint probability density of eigenvalues for such an induced Ginibre ensemble and study various spectral correlation functions for complex and real matrices, and analyse universal behaviour in the limit of large dimensions. In this limit, the eigenvalues of the induced Ginibre ensemble cover uniformly a ring in the complex plane. The real induced Ginibre ensemble is shown to be useful to describe the statistical properties of evolution operators associated with random quantum operations for which the dimensions of the input state and the output state do differ.

PACS numbers: 02.10.Yn, 02.50.-r, 03.65.Ta, 03.67.-a

1. Introduction

In 1965 Ginibre introduced a new threefold family of non-Hermitian Gaussian random matrix ensembles as an extension to the mathematical theory of Hermitian random matrices [1]. Since then, Ginibre ensembles of random matrices have found numerous applications in various fields of physics. They can be used to describe non-unitary dynamics of open quantum systems [2], transfer matrices in mesoscopic wires [3] and directed quantum chaos [4]. Real non-symmetric random matrices can be used in mathematical finances to describe correlations between time series of prices of various stocks [5, 6] and in physiology to characterize correlations between data representing the electric activity of the brain [7, 8]. The same ensemble of real Ginibre

matrices describes spectral properties of evolution operators representing random quantum operations [9] and is useful in telecommunications to characterize scattering of electromagnetic waves on random obstacles [10], and to describe the effects of synchronization in random networks [11].

In his original paper, Ginibre derived the eigenvalue distribution of matrices with i.i.d. real, complex or quaternion-real entries [1]. These Ginibre ensembles are sometimes denoted in the literature [12] as GinOE, GinUE and GinSE, respectively. The letters U, O and S stand for orthogonal, unitary and symplectic symmetry class. The case GinOE of real asymmetric matrices proved to be the hardest and Ginibre studied only the special case that all eigenvalues are real.

It took another 25 years for Lehmann and Sommers [13] and Edelman [14] to derive the complete distribution of eigenvalues for the real Ginibre ensemble. Further difficulty arose in the computation of the eigenvalue correlation functions. In 2007, Akemann and Kanzieper succeeded in expressing the smooth complex correlation functions as Pfaffians [15], whereas Sinclair presented a method for averaging over the real Ginibre ensemble in terms of Pfaffians [12]. Finally, Forrester and Nagao were able to determine the real–real as well as the complex–complex correlation functions as Pfaffians using the method of skew-orthogonal polynomials [16, 17], while Borodin and Sinclair gave the real–complex correlation in addition to a thorough asymptotic analysis [18]. Simultaneously and independently, Sommers [19] and Sommers and Wierczonek [20] derived the complex–complex, real–real and complex–real eigenvalue correlation functions via free-fermion diagram expansion. Similar progress was made for the chiral real Gaussian ensemble [21] (see also [22, 23] for the chiral complex and quaternion-real Gaussian ensembles) and for two non-Gaussian ensembles of real asymmetric matrices [24, 25]. A general review on non-Hermitian random matrices can be found in [26], while a recent overview on the Ginibre ensembles is provided in [27].

A square matrix A of size N pertaining to the complex (real) *Ginibre ensemble* consists of N^2 independent complex (real) random numbers drawn from a normal distribution with zero mean and a fixed variance [28]. Normalizing to $\langle \text{Tr} AA^\dagger \rangle = N^2$, the joint probability density function of the matrix entries in this ensemble is

$$p_G(A) \propto \exp\left(-\frac{\beta}{2} \text{Tr} A^\dagger A\right), \quad (1)$$

where $\beta = 1$ for real matrices and $\beta = 2$ for complex matrices. A^\dagger is the Hermitian conjugate of A which for the real matrices is simply the transpose of A . Note that the same formula can also be used to define an analogous probability measure in the space of rectangular matrices A . The spectral density of the Ginibre ensemble is described by the Girko circular law [29] according to which the eigenvalue distribution for large N is, in the leading order, uniform in a disc about the origin in the complex plane [30–32].

The Ginibre ensemble was generalized by Feinberg and Zee [33, 34] who studied random complex matrices with joint probability density of matrix entries

$$p_{FZ}(A) \propto \exp(-\text{Tr} V(A^\dagger A)), \quad (2)$$

where $V(A^\dagger A)$ is a polynomial in $A^\dagger A$. It was found in [33, 34] that in the limit of large matrix dimensions, the spectral measure of (2) can only be supported by a single ring (or disc) on the complex plane. A mathematical proof of the ‘single ring theorem’ was recently provided by Guionnet *et al* [35] who considered random matrices $A = UDV$ with independent Haar unitary U and V , and real diagonal D ; see also [36, 37] for an alternative approach. The Feinberg–Zee ensemble (2) fits into this scheme on making use of the singular value decomposition in (2). This is because the corresponding Jacobian depends only on the singular values of A , see, e.g., [38]. The matrices considered in [36, 37] are of the form $A = UD$ with the Haar unitary U

and diagonal D ; however, as far as eigenvalues are concerned, the two ensembles UDV and UD are equivalent because of the invariance of the Haar measure. Yet another approach to obtaining the spectral measure of products of random matrices was proposed in [39, 40] and extended to weighted sums of unitary matrices in [41].

In this work, we study a generalization of the Ginibre ensemble of $N \times N$ matrices, complex ($\beta = 2$) or real ($\beta = 1$), specified by the probability distribution with density

$$p_{\text{IndG}}^{(\beta)}(G) = C_L^{(\beta)} (\det G^\dagger G)^{\frac{\beta}{2}L} \exp\left(-\frac{\beta}{2} \text{Tr} G^\dagger G\right) \quad (3)$$

with the normalization constant

$$C_L^{(\beta)} = \pi^{-\frac{\beta}{2}N^2} \left(\frac{\beta}{2}\right)^{\frac{1}{2}N^2 - \frac{1}{2}NL} \prod_{j=1}^N \frac{\Gamma(\frac{\beta}{2}j)}{\Gamma(\frac{\beta}{2}(j+L))}. \quad (4)$$

Here L is a free parameter such that $L \geq 0$. Formally, the random matrix ensemble (3) is a special case of the Feinberg–Zee ensemble (2) corresponding to the potential $V(t) = -\frac{\beta}{2}(t - L \log t)$. This specific choice of potential makes the model exactly solvable in which one is able to obtain the joint probability density function of eigenvalues and, consequently, study the eigenvalue statistics to the same level of detail as in the original Ginibre ensemble. For example, the distribution of the real eigenvalues for real matrices and all eigenvalue correlation functions become accessible. Obtaining this information by the techniques used to study the Feinberg–Zee ensemble seems to be hardly possible.

Ensemble (3) will be called the induced Ginibre ensemble, as we will show in section 2 that a random matrix G from this ensemble can be generated out of an auxiliary rectangular Gaussian matrix X of size $(N+L) \times N$ and a random unitary matrix distributed according to the Haar measure on the unitary group. Thus, the Gaussian measure on the space of $(N+L) \times N$ rectangular matrices is used to induce another measure in the space of square $N \times N$ matrices. A similar construction is used to generate ensembles of quantum states [42], as the Haar measure on the group of unitary matrices of size kN induces a probability measure in the space of mixed quantum states of size N . Random square matrices of size N from the induced ensemble can also be obtained by means of quadratization (5) of rectangular $(N+L) \times N$ random matrices.

The induced Ginibre ensemble of real non-symmetric matrices can be defined in an analogous way. We study spectral density and eigenvalue correlation functions for both induced ensembles of random matrices. We show that the induced Ginibre ensemble exhibits interesting behaviour in the limit of large matrix dimensions: its eigenvalues spreading across an annulus in the complex plane, as opposed to the circular law. Secondly, on the level of correlation functions our asymptotic analysis reveals Ginibre correlations, supporting the universality conjecture.

This paper is organized as follows. In section 2, we introduce a procedure for quadratization of rectangular matrices and derive the induced Ginibre distribution. In section 3, the induced Ginibre ensemble of complex matrices is investigated, its spectral density is derived and eigenvalue correlation functions are analysed. Section 4 is devoted to the induced Ginibre ensemble of real matrices. In section 5, it is demonstrated that the real induced Ginibre ensemble can be linked to evolution operators associated with generic complementary quantum operations, which modify the dimensionality of the quantum system. Proofs of technical results are relegated to the appendices.

2. Quadraticization of rectangular matrices and induced Ginibre ensembles

Consider complex or real rectangular matrices X with M rows and N columns. We will assume that $M > N$, so that our rectangular matrices are ‘standing’. Let Y and Z denote, respectively, the upper square block of size $N \times N$ and the lower rectangular block of size $(M - N) \times N$ of the matrix X . Since the standard definition of the spectrum does not work for non-square matrices, we provide a unitary transformation $W \in U(M)$ intended to set the lower block Z to zero:

$$W^\dagger X = W^\dagger \begin{bmatrix} Y \\ Z \end{bmatrix} = \begin{bmatrix} G \\ 0 \end{bmatrix}. \tag{5}$$

One can easily find such transformations. Assuming that the matrix X has rank N , consider the linear span \mathcal{S} of the column vectors of X . Let $\mathbf{q}_1, \dots, \mathbf{q}_N$ be an orthonormal basis in \mathcal{S} and $\mathbf{q}_{N+1}, \dots, \mathbf{q}_M$ be an orthonormal basis in \mathcal{S}^\perp , the orthogonal complement of \mathcal{S} in \mathbb{C}^M . If we set $W = [\mathbf{q}_1 \dots \mathbf{q}_M]$, then (5) holds. Obviously, all other suitable unitary transformations are obtained from this W by multiplying it to the right by the block diagonal unitary matrices $\text{diag}[U, V]$ where U and V run through the unitary groups $U(N)$ and $U(M - N)$, respectively. Multiplying W by $\text{diag}[\mathbb{1}_N, V]$ corresponds to choosing a different orthonormal basis in \mathcal{S}^\perp , and multiplying W by $\text{diag}[U, \mathbb{1}_{M-N}]$ corresponds to replacing the matrix G by UG .

It is straightforward to check that any unitary matrix $W \in U(M)$ can be transformed into the block form

$$W = \begin{bmatrix} (\mathbb{1}_N - CC^\dagger)^{1/2} & C \\ -C^\dagger & (\mathbb{1}_{M-N} - C^\dagger C)^{1/2} \end{bmatrix}, \quad \text{where } C \text{ is } N \times (M - N), \tag{6}$$

by multiplying it to the right by the block diagonal unitary matrix as above⁵. Correspondingly, we will seek the unitary matrix W in (5) in the block form (6). This additional condition makes the decomposition in (5) unique for ‘standing’ rectangular matrices of full rank. Note that if the matrix X is real then G, W and, correspondingly, C in (6) can all be chosen real as well.

Having settled on the choice of W , we can solve the equation in (5) for G and C .

Lemma 2.1. *Let $M > N$. Suppose that Y is $N \times N$ and Z is $(M - N) \times N$, and Y is invertible. Then, there is a unique $M \times M$ unitary matrix W of the form (6) such that (5) holds. The square matrix G in (5) is given by*

$$G = \left(\mathbb{1}_N + \frac{1}{Y^\dagger} Z^\dagger Z \frac{1}{Y} \right)^{1/2} Y. \tag{7}$$

A direct calculation proving this lemma is provided in appendix A.

We now have a procedure for quadraticizing ‘standing’ rectangular matrices. Of course, in the opposite case of ‘lying’ rectangular matrices ($M < N$) one may apply the same procedure to quadraticize the transposed matrix X^T . Thus, any rectangular matrix X can be quadraticized by a unitary transformation on its columns (or rows, if the number of columns is greater than the number of rows), giving rise to a square matrix G . As G is a unique solution of equation (5), its spectrum characterizes algebraic properties of the rectangular matrix X .

Motivated by studies of quantum operations, see section 5, we want to explore the concept of quadraticization in the context of random rectangular matrices. To this end, we will consider

⁵ Representation (6) can also be derived by exponentiating matrices of the form $\mathcal{A} = \begin{bmatrix} 0 & A \\ -A^\dagger & 0 \end{bmatrix}$ with A being $N \times (M - N)$. Such matrices \mathcal{A} form the orthogonal component of $\mathfrak{u}(N) \oplus \mathfrak{u}(M - N)$ in $\mathfrak{u}(M)$; hence, the matrices $W = \exp(\mathcal{A})$ provide a natural set of representatives for $U(M)/(U(N) \times U(M - N))$. Expanding the exponential in the Taylor series leads to (6) with $C = A(A^\dagger A)^{-1/2} \sin((A^\dagger A)^{1/2})$.

Gaussian random matrices X , real or complex, with M rows and N columns, $M > N$, so that the probability distribution of X is specified by the measure

$$d\nu(X) \propto \exp\left(-\frac{\beta}{2} \text{Tr} X^\dagger X\right) |dX|, \quad (8)$$

where $\beta = 1$ or $\beta = 2$ depending on whether the matrix X is real or complex, and $|dX|$ is the flat (Lebesgue) measure on the corresponding matrix space.

Note that the result of quadratization depends on the particular choice of elements of $W^\dagger X$ which are set to zero by action of the unitary W in the ansatz (5). For instance, one could define another matrix G' by assuming that unitary W brings to zero the upper rectangular part of the matrix $W^\dagger X$. However, we are going to apply (7) for a random matrix X , drawn from a unitary invariant Gaussian ensemble. Thus, the statistical properties of G and G' will be the same. Therefore, for a rectangular random Gaussian matrix X one may associate by (7) a square random matrix G , which we will call the *quadratization* of X .

The probability distribution for square matrices G (7) induced by the normal distribution for Y and Z can be obtained directly from (5). However, it is useful to look at this problem from the singular value decomposition (SVD) perspective, especially as one can utilize the known Jacobian of the corresponding coordinate transformation.

Ignoring a set of zero probability measure, the $N \times N$ matrix $X^\dagger X$ has N distinct eigenvalues s_j , $0 < s_1 < s_2 < \dots < s_N$, and the SVD asserts that X can be factorized as follows:

$$X = Q \Sigma^{1/2} P^\dagger, \quad (9)$$

where $\Sigma = \text{diag}(s_1, \dots, s_N)$, and Q and P are, respectively, $M \times N$ and $N \times N$ matrices with orthonormal columns, so that $Q^\dagger Q = P^\dagger P = \mathbb{1}_N$. The columns of P are in fact eigenvectors of $X^\dagger X$ and, hence, are defined up to phase factor (or sign for real matrices). To make the choice of P unique, we will impose the condition that the first non-zero entry in each column of P is positive. Consequently, the matrix Q is also defined uniquely via $Q = X P \Sigma^{-1/2}$. Thus, factorization (9) introduces a new coordinate system (Q, P, Σ) in the space of rectangular matrices. In the new coordinates [38],

$$d\nu(X) = d\mu(Q) d\tilde{\mu}(P) d\sigma(\Sigma), \quad (10)$$

where $d\mu(Q)$ is the normalized invariant (Haar) measure on the (Stiefel) manifold of complex (or, correspondingly, real) $M \times N$ matrices with orthonormal columns, $d\tilde{\mu}(P)$ is the normalized measure defined by the maximum degree form

$$\omega(P) = \begin{cases} \wedge_{1 \leq k < j \leq N} (\text{Re}(P^\dagger dP)_{jk} \wedge \text{Im}(P^\dagger dP)_{jk}) & (\beta = 2), \\ \wedge_{1 \leq k < j \leq N} (P^\dagger dP)_{jk} & (\beta = 1), \end{cases}$$

on the manifold of unitary (real orthogonal for $\beta = 1$) $N \times N$ matrices satisfying the column condition above (the first non-zero entry in each column is positive), and

$$d\sigma(\Sigma) \propto (\det \Sigma)^{\frac{\beta}{2}(M-N+1-\frac{2}{\beta})} e^{-\frac{\beta}{2} \text{Tr} \Sigma} \prod_{j < k} |s_k - s_j|^\beta \prod_{j=1}^N ds_j. \quad (11)$$

It is apparent from (10) that the matrices Q , P and Σ are mutually independent.

Let us introduce an additional unitary (real orthogonal for $\beta = 1$) matrix U of size $N \times N$ and rewrite (9) in the form

$$X = Q U U^\dagger \Sigma^{1/2} P^\dagger = Q U G. \quad (12)$$

The matrix $G = U^\dagger \Sigma^{1/2} P^\dagger$ is $N \times N$. Now choose U to be Haar unitary (real orthogonal for $\beta = 1$) and independent of Q , P and Σ . Then, by rolling back from (11) to (9) with Q replaced by U^\dagger , the square matrix G is distributed according to the measure

$$d\mu_{\text{Ind}G}(G) \propto (\det G^\dagger G)^{\frac{\beta}{2}(M-N)} \exp\left(-\frac{\beta}{2} \text{Tr} G^\dagger G\right) |dG|, \quad (13)$$

with the determinant on the right in (13) originating from the one in (11). This is the induced Ginibre distribution introduced in section 1. Because of the invariance of the Haar distribution, the unitary matrix U in (12) can be absorbed into Q . In other words, we have decomposed the rectangular Gaussian X into the product

$$X = \tilde{Q}G \tag{14}$$

of two independent random matrices: the rectangular matrix $\tilde{Q} := QU$ with orthonormal columns, which has a uniform distribution, and a square matrix G , which has an induced Ginibre distribution. Decomposition (14) can also be written as

$$X = W \begin{bmatrix} G \\ 0 \end{bmatrix}, \tag{15}$$

where W is an $M \times M$ unitary (real orthogonal for $\beta = 1$) matrix obtained from the $M \times N$ matrix \tilde{Q} by appending suitable column vectors. This is nothing else than equation (5). One can transform the matrix W to the block form of (6), so that (15) becomes

$$X = \begin{bmatrix} (\mathbb{1}_N - CC^\dagger)^{1/2} & C \\ -C^\dagger & (\mathbb{1}_{M-N} - C^\dagger C)^{1/2} \end{bmatrix} \begin{bmatrix} \tilde{G} \\ 0 \end{bmatrix},$$

where $\tilde{G} = \tilde{U}G$ for some unitary \tilde{U} . Obviously, \tilde{G} has the same distribution as G . Thus,

Lemma 2.2. *Suppose that X is $M \times N$ Gaussian, $M > N$, with distribution (8). Then, its quadratization G has the induced Ginibre distribution (13).*

This result holds in the cases of complex and real Ginibre matrices. It shows that the notion of quadratization of a rectangular matrix is specially justified for Gaussian rectangular matrices. In this case, the statistical properties of the outcome do not depend on the particular way in which the quadratization is obtained out of the initially rectangular random matrix. This is in a clear analogy to the ensembles of truncations of unitary [43] and orthogonal [25] random matrices, the statistical properties of which do not depend on the choice of the rows and columns to be truncated. Thus, for any random rectangular matrix X we may introduce its *quasi-spectrum* as the spectrum of its quadratization.

Lemma 2.2 together with lemma 2.1 provides a recipe for generating matrices from the induced Ginibre distribution starting with Gaussian matrices. Interestingly, by rearranging (12), one obtains another recipe which might be less efficient computationally but still interesting from the theoretical point of view. Indeed, since $(X^\dagger X)^{1/2} = P\Sigma^{1/2}P^\dagger$, it follows from (12) that

$$G = U^\dagger Q^\dagger X = U^\dagger P^\dagger (X^\dagger X)^{1/2} = \tilde{U}^\dagger (X^\dagger X)^{1/2}, \quad \text{where } \tilde{U} = PU. \tag{16}$$

Recalling that the Haar measure is invariant with respect to right (and left) multiplication, one arrives at the following recipe for generating matrices from the induced Ginibre distribution.

Lemma 2.3. *Suppose that U is $N \times N$ Haar unitary (real orthogonal for $\beta = 1$) and X is $M \times N$ Gaussian with distribution (8) and independent of U . Then, the $N \times N$ matrix $G = U(X^\dagger X)^{1/2}$ has the induced Ginibre distribution (13).*

Obviously, our arguments extend to random rectangular matrices with invariant distributions other than Gaussian, e.g. the Feinberg–Zee distribution with density

$$p_{\text{FZ}}(X) \propto \exp[-\text{Tr} V(X^\dagger X)], \tag{17}$$

where X is $M \times N$, $M > N$. On applying the procedure of quadratization to such an ensemble, one obtains the induced Feinberg–Zee distribution

$$p_{\text{IndFZ}}(G) \propto (\det G^\dagger G)^{\frac{\beta}{2}(M-N)} \exp[-\text{Tr} V(G^\dagger G)].$$

Another example is provided by rectangular truncations of random unitary or orthogonal matrices⁶. By applying quadratization, one can extend the study of square truncations of Haar unitary [43] and orthogonal [25] matrices.

In the context of eigenvalue maps, it is instructive to embed rectangular $M \times N$ matrices X into the space of $M \times M$ matrices by augmenting X with $M - N$ zero column vectors and write the quadratization rule (5) in terms of square matrices albeit with zero blocks:

$$W^\dagger \tilde{X} = \tilde{G}, \quad \text{with } \tilde{X} = \begin{bmatrix} Y & 0 \\ Z & 0 \end{bmatrix} \quad \text{and} \quad \tilde{G} = \begin{bmatrix} G & 0 \\ 0 & 0 \end{bmatrix}, \quad (18)$$

where as before W is $M \times M$ unitary, Y and G are $N \times N$ and Z is $(M - N) \times N$.

By construction, zero is an eigenvalue of \tilde{X} of multiplicity $M - N$ and the remaining N eigenvalues of \tilde{X} are exactly those of its top left block Y . Thus, our quadratization procedure induces an eigenvalue map: the eigenvalues of \tilde{X} are mapped onto the eigenvalues of \tilde{G} . Under this map, the zero eigenvalue stays put, and its multiplicity is conserved, and, otherwise, the eigenvalues of Y are mapped onto those of G .

For Gaussian matrices, the eigenvalues of Y for large matrix dimensions ($M \gg 1$ and $N \propto M$) are distributed uniformly in a disc, and we will show in the subsequent sections that the eigenvalues of G are distributed uniformly in a ring. This hole in the spectrum created by quadratization can be interpreted as due to repulsion of eigenvalues of \tilde{G} from its zero eigenvalues.

3. Complex induced Ginibre ensemble

The complex induced Ginibre ensemble is defined by the probability density $p_{\text{IndG}}^{(2)}(G)$ (3)–(4) on the set of complex $N \times N$ matrices $G = [g_{jk}]$ with the volume element $|dG| = \prod_{j,k=1}^N d\text{Re } g_{jk} d\text{Im } g_{jk}$. In the subsequent analysis, we restrict ourselves to the non-negative integer L , in which case the obtained results can be interpreted in the context of quadratization of $M \times N$ matrices with $L = M - N$ being a measure of rectangularity as was discussed in section 2. However, our analysis extends almost verbatim to real non-negative L , see [45].

The symmetrized joint probability density function $P(\lambda_1, \dots, \lambda_N)$ of the eigenvalues in the complex induced Ginibre ensemble is obtained from that in the Ginibre ensemble [1, 28] by multiplying through by $\det(GG^\dagger)^L = \prod_{j=1}^N |\lambda_j|^{2L}$ and re-evaluating the normalization constant. This yields

$$P(\lambda_1, \dots, \lambda_N) = \frac{1}{N! \pi^N} \prod_{j=1}^N \frac{1}{\Gamma(j+L)} \prod_{j < k} |\lambda_k - \lambda_j|^2 \prod_{j=1}^N |\lambda_j|^{2L} \exp\left(-\sum_{j=1}^N |\lambda_j|^2\right). \quad (19)$$

Consequently, the n -eigenvalue correlation functions

$$R_n(\lambda_1, \dots, \lambda_n) = \frac{N!}{(N-n)!} \int P(\lambda_1, \dots, \lambda_N) d^2\lambda_{n+1} \dots d^2\lambda_N$$

follow in the determinantal form

$$R_n(\lambda_1, \dots, \lambda_n) = \det\left(K_N(\lambda_k, \lambda_l)\right)_{k,l=1}^n \quad (20)$$

via the method of orthogonal polynomials in the same way as for the complex Ginibre ensemble [28]. The kernel $K_N(\lambda_k, \lambda_l)$ is given by

$$K_N(\lambda_k, \lambda_l) = \frac{1}{\pi} e^{-\frac{1}{2}|\lambda_k|^2 - \frac{1}{2}|\lambda_l|^2} \sum_{j=0}^{N-1} \frac{(\lambda_k \bar{\lambda}_l)^{j+L}}{\Gamma(j+L+1)}. \quad (21)$$

⁶ For a range of parameter values, the matrix distribution of such truncations is given by (17) with $V(X^\dagger X)$ replaced by a sum of powers of $\log X^\dagger X$ and $\log(1 - X^\dagger X)$, see [44].

It should be noted that the right-hand side in (21) can be expressed as a difference of two incomplete gamma functions. This makes the asymptotic analysis of the eigenvalue statistics for large matrix dimensions straightforward.

Of special interest is the mean eigenvalue density $\rho_N(\lambda) := R_1(\lambda) = K_N(\lambda, \lambda)$,

$$\rho_N(\lambda) = \frac{1}{\pi} e^{-|\lambda|^2} \sum_{l=L}^{L+N-1} \frac{|\lambda|^{2l}}{l!} = \frac{1}{\pi} \left[\frac{\gamma(L, |\lambda|^2)}{\Gamma(L)} - \frac{\gamma(L+N, |\lambda|^2)}{\Gamma(L+N)} \right], \quad (22)$$

where $\gamma(a, z)$ is the lower incomplete gamma function [46]

$$\gamma(a, z) := \int_0^z t^{a-1} e^{-t} dt. \quad (23)$$

In the limit when N is large and $L = N\alpha$, $\alpha > 0$ (which corresponds to quadratization of ‘standing’ rectangular matrices of size $(N + L) \times N$), the eigenvalue distribution (in the leading order) is uniform and supported by a ring about the origin with the inner and outer radii $r_{\text{in}} = \sqrt{L}$ and $r_{\text{out}} = \sqrt{L + N}$, respectively. More precisely,

$$\lim_{N \rightarrow \infty} \rho_N(\sqrt{N}z) = \frac{1}{\pi} [\Theta(\sqrt{\alpha + 1} - |z|) - \Theta(\sqrt{\alpha} - |z|)], \quad (24)$$

where Θ is the Heaviside function, $\Theta(x) = 1$ if $x > 0$, $\Theta(x) = 0$ if $x < 0$ and $\Theta(0) = \frac{1}{2}$.

Close to the circular edges of the eigenvalue support, for every angle ϕ ,

$$\lim_{N \rightarrow \infty} \rho_N((r_{\text{out}} + \xi) e^{i\phi}) = \lim_{N \rightarrow \infty} \rho_N((r_{\text{in}} - \xi) e^{i\phi}) = \frac{1}{2\pi} \operatorname{erfc}(\sqrt{2}\xi), \quad (25)$$

where $\operatorname{erfc}(x)$ is the complementary error function:

$$\operatorname{erfc}(x) := \frac{2}{\sqrt{\pi}} \int_x^\infty e^{-t^2} dt. \quad (26)$$

Hence, the eigenvalue density falls from $1/\pi$ to zero at a Gaussian rate at the inner and outer boundaries of the eigenvalue support. As was observed in [37], the scaling law (25) is universal; see equations (42)–(43) in [37].

The scaling limits of the eigenvalue correlation functions $R_n(\lambda_1, \dots, \lambda_n)$ in the induced Ginibre ensemble can also be obtained from (20)–(21). Not surprisingly in the regime when $N \rightarrow \infty$ and $L \propto N$, one recovers the same expressions as in the Ginibre ensemble [1, 18, 47], both in the bulk and at the circular edges of the eigenvalue distribution; see appendix C.

A quick inspection of the joint probability density function (jpdf) of the eigenvalues (19) convinces that the determinantal power in front of the Gaussian weight in (3) repels eigenvalues from the origin. When the rectangularity index L grows proportionally with N , the eigenvalues are actually displaced from the origin, resulting in the creation of a ring of eigenvalues; see figure 1.

In the context of the augmented matrix \tilde{G} (18), the creation of the hole in the spectrum can be interpreted as due to repulsion from zero eigenvalues. There are $M - N$ eigenvalues of \tilde{G} located at the origin and the remaining eigenvalues are exactly as those of G . When L increases, the zero eigenvalues become dominant and repel the rest of the eigenvalues strongly, which leads to the creation of the hole in the spectrum. Looking at the polynomial on the right-hand side in (22), it starts with the power $|\lambda|^{2L}$ and ends with the power $|\lambda|^{2(N+L-1)} = |\lambda|^{2(M-1)}$. Also in the 2-dim plot in the complex plane, we see that $(M - N)$ eigenvalues have been taken off from the centre near the origin and put in the top of the surface of the circle of support. Thus, the outer radius of the support of the density increases from \sqrt{N} to \sqrt{M} while there is an inner hole of radius $\sqrt{L} = \sqrt{M - N}$ —see figure 1.

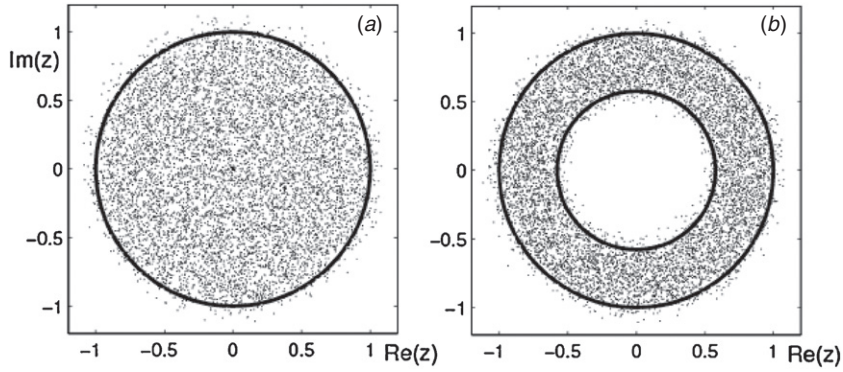


Figure 1. Spectra of matrices pertaining to the induced Ginibre ensemble of complex matrices for dimension $N = 128$ and (a) $L = 0$ and (b) $L = 32$. Each plot consists of data from 128 independent realizations. The spectra are rescaled by a factor of $1/\sqrt{N+L}$ to be localized inside the unit disc. The circles of radius $r_{\text{in}} = \sqrt{L/(N+L)}$ (inner one) and $r_{\text{out}} = 1$ (outer one) are depicted to guide the eye.

Now we will explore a different regime when the rectangularity index $L = M - N \ll N$. This corresponds to the quadratization of almost square matrices. In the vicinity of the origin, the corresponding large- N (or equivalently large- M) limit can be performed by simply extending the summation in (21) to infinity. For the mean eigenvalue density, $\rho_N(\lambda) = R_1(\lambda)$, it gives⁷

$$\lim_{N \rightarrow \infty} \rho_N(\lambda) = \frac{1}{\pi} e^{-|\lambda|^2} \sum_{j=0}^{\infty} \frac{|\lambda|^{2(j+L)}}{\Gamma(j+L+1)} = \frac{1}{\pi} \frac{\gamma(L, |\lambda|^2)}{\Gamma(L)}$$

and more generally

$$\lim_{N \rightarrow \infty} R_n(\lambda_1, \dots, \lambda_n) = \det \left(K_{\text{origin}}(\lambda_j, \lambda_k) \right)_{j,k=1}^n, \tag{27}$$

with

$$K_{\text{origin}}(\lambda_j, \lambda_k) = \frac{1}{\pi} \frac{\gamma(L, \lambda_j \bar{\lambda}_k)}{\Gamma(L)} = \frac{1}{\pi} \frac{1}{\Gamma(L)} \int_0^{\lambda_j \bar{\lambda}_k} t^{L-1} e^{-t} dt. \tag{28}$$

At the origin, the eigenvalue density vanishes algebraically, $\rho_N(\lambda) \sim \frac{1}{\pi} \frac{|\lambda|^{2L}}{\Gamma(L+1)}$ as $\lambda \rightarrow 0$, uniformly in N . Away from the origin, the density reaches its asymptotic value $1/\pi$ very quickly⁸. This plateau extends to a full circle of radius \sqrt{N} :

$$\lim_{N \rightarrow \infty} \rho_N(\sqrt{N}z) = \frac{1}{\pi} \Theta(1 - |z|),$$

as in the Ginibre ensemble and, moreover, for reference points $\sqrt{N}u$, $|u| < 1$, one also recovers the Ginibre correlations.

⁷ The complex induced Ginibre ensemble is a special case of the more general non-Hermitian random matrix ensemble studied by Akemann in [48]. Correspondingly, our (27)–(28) is a limiting case of equation (4.5) in [48]. Taking the corresponding limit is straightforward for small values of L .

⁸ A similar behaviour is found in the chiral Ginibre ensemble; see [49] for a discussion in the context of gap probabilities.

Another quantity of interest is the so-called hole probability $A(s)$ at the origin giving the probability that no eigenvalues lie inside the disc $D_s = \{z : |z| < s\}$. For finite N , the hole probability $A(s)$ can be derived from the expression

$$A(s) = \int P(\lambda_1, \dots, \lambda_N) \prod_{j=1}^N (1 - \chi_{D_s}(\lambda_j)) d^2\lambda_1 \dots d^2\lambda_N,$$

where χ_{D_s} denotes the indicator function of D_s by employing the method of orthogonal polynomials to yield

$$A(s) = \prod_{j=1}^N \frac{\Gamma(j + L, s^2)}{\Gamma(j + L)} \tag{29}$$

with $\Gamma(a, x) := \int_x^\infty e^{-t} t^{a-1} dt$ denoting the upper incomplete gamma function. In the asymptotic regime of almost square matrices, taking the large N limit, while keeping L fixed, results in the easily accessible expression for the hole probability $A(s) = 1 - \frac{s^{2(L+1)}}{(L+1)!} + O(\frac{s^{2(L+2)}}{(L+2)!})$.

4. Real induced Ginibre ensemble

The real induced Ginibre ensemble is defined by the probability density $p_{\text{IndG}}^{(1)}(G)$ (3)–(4) on the set of real $N \times N$ matrices $G = [g_{jk}]$ with the volume element $|dG| = \prod_{j,k=1}^N dg_{jk}$. In the following, we restrict ourselves to even dimension N .

4.1. The joint distribution of eigenvalues

The difficulty in deriving the joint probability density function for real asymmetric matrices is due to the fact that there is a non-zero probability $p_{N,k}$ for the matrix G to have k real eigenvalues. In the following, it is assumed that G has k real ordered eigenvalues: $\lambda_1 \geq \dots \geq \lambda_k$, while $l = \frac{N-k}{2}$ denotes the number of complex conjugate eigenvalue pairs $x_1 \pm iy_1, \dots, x_l \pm iy_l$ ordered by their real part. We adopt the convention that $y_j > 0$ for all j . In the case of two complex eigenvalues with identical real part, the eigenvalue pairs are ordered by the imaginary part.

As a consequence, the eigenvalue jpdf decomposes into a sum of probability densities $P_{N,k,l}(\lambda_1, \dots, \lambda_k, x_1 + iy_1, \dots, x_l + iy_l)$, corresponding to having k real eigenvalues and l pairs of complex conjugate eigenvalues. In order for $P_{N,k,l}$ to be non-zero, k must be even, as it is assumed that N is even.

The derivation of the eigenvalue jpdf goes as follows [14]; see [13, 20, 27] for alternative derivations. In order to change variables from the entries of G to the eigenvalues of G and some auxiliary variables, the real Schur decomposition is employed: $G = QTQ^T$, where $Q \in \mathbb{R}^{N \times N}$ is an orthogonal matrix, whose first row is chosen to be non-negative and the matrix $T \in \mathbb{R}^{N \times N}$ is block triangular in the form

$$T = \begin{pmatrix} \lambda_1 & \cdots & t_{1k} & t_{1,k+1} & \cdots & t_{1,N} \\ & \ddots & \vdots & \vdots & & \vdots \\ 0 & & \lambda_k & t_{k,k+1} & \cdots & t_{k,N} \\ 0 & \cdots & 0 & Z_1 & \cdots & t_{k+1,N} \\ \vdots & & \vdots & & \ddots & \vdots \\ 0 & \cdots & 0 & 0 & & Z_l \end{pmatrix} = \begin{pmatrix} \Lambda & T^U \\ 0 & Z \end{pmatrix}.$$

Here Λ is triangular containing the real eigenvalues $\lambda_1, \dots, \lambda_k$ of G on its diagonal and Z is block triangular containing the 2×2 blocks:

$$Z_j = \begin{pmatrix} x_j & b_j \\ -c_j & x_j \end{pmatrix}, \quad b_j c_j > 0, \quad b_j \geq c_j \quad \text{and} \quad y_j = \sqrt{b_j c_j}$$

on its block diagonal.

The Jacobian of this change of variable was already computed in [14]:

$$|J| = 2^l \left| \Delta(\{\lambda_j\}_{j=1, \dots, k} \cup \{x_j \pm iy_j\}_{j=1, \dots, l}) \right| \prod_{i>k} (b_i - c_i),$$

with $\Delta(\{z_p\}_{p=1, \dots, n}) := \prod_{i<j} (z_j - z_i)$ denoting the Vandermonde determinant. Consequently, we arrive at the relation

$$\begin{aligned} p_{\text{IndG}}^{(1)}(G) |dG| &= C_L |J| \prod_{j=1}^k |\lambda_j|^L \prod_{m=1}^l (x_m^2 + b_m c_m)^L \\ &\times e^{-\frac{1}{2} \sum_{j=1}^k \lambda_j^2 - \frac{1}{2} \sum_{i,j} t_{ij}^2 - \sum_{j=1}^l (x_j^2 + \frac{b_j^2}{2} + \frac{c_j^2}{2})} |dO| |d\Lambda| |dT^U| |dZ|. \end{aligned}$$

Here, $|dO|$ denotes the volume form on the space of orthogonal $N \times N$ matrices with positive first row while $|d\Lambda| = \prod_{j=1}^k d\lambda_j \prod_{m<n \leq k} dt_{mn}$, $|dT^U| = \prod_{m=1, \dots, k, n=k+1, \dots, N} dt_{mn}$ and $|dZ| = \prod_{j=1}^l db_j dc_j dx_j \prod_{m, n=k+1}^N dt_{mn}$. In addition, another change of variable is necessary from the entries x_j, b_j, c_j of the matrix blocks Z_j to the real and imaginary part x_j, y_j of the complex conjugate eigenvalue pairs and an auxiliary variable δ_j . The change of variable is performed in the following way:

$$\text{set} \quad b_j = \frac{1}{2} (\delta_j + \sqrt{\delta_j^2 + 4y_j^2}) \quad \text{and} \quad c_j = \frac{1}{2} (-\delta_j + \sqrt{\delta_j^2 + 4y_j^2}), \quad (30)$$

which implies $y_j = \sqrt{b_j c_j}$ and $\delta_j = b_j - c_j$. The Jacobian of this second change of variables can easily be determined:

$$|\bar{J}| = \frac{4y_j}{\sqrt{\delta_j^2 + 4y_j^2}}.$$

Integrating out the auxiliary variables δ_j for $j = 1, \dots, m$ and t_{ij} as well as using $\text{Vol}(O[N]) = \frac{\pi^{\frac{1}{4}N(N+1)}}{\prod_{j=1}^N \Gamma(\frac{j}{2})}$ finally yields the partial eigenvalue joint probability density function:

$$\begin{aligned} P_{N,k,l}(\lambda_1, \dots, \lambda_k, x_1 + iy_1, \dots, x_l + iy_l) &= \frac{2^{2l - \frac{1}{4}N(N+1)} \pi^{-NL}}{\prod_{j=1}^N \Gamma(\frac{L+j}{2})} \left| \Delta(\{\lambda_j\}_{j=1}^k \cup \{x_j \pm iy_j\}_{j=1}^l) \right| \\ &\times \prod_{j=1}^k |\lambda_j|^L e^{-\frac{1}{2}|\lambda_j|^2} \prod_{m=1}^l (x_m^2 + y_m^2)^L e^{y_m^2 - x_m^2} y_m \text{erfc}(\sqrt{2}y_m), \end{aligned}$$

where $\text{erfc}(x)$ is the complementary error function (26), $\lambda_j \in \mathbb{R}$ for $j = 1, \dots, k$ and $x_m + iy_m \in \mathbb{C}_+$ for $m = 1, \dots, l$. Integrating the partial eigenvalue jpdf $P_{N,k,l}$ over $\mathbb{R}^k \times \mathbb{C}_+^{2l}$ gives $p_{N,k}$.

4.2. The (K', L') -correlation functions

Again we are interested in the correlations between the eigenvalues. The first starting point is the (K', L', k', l') -partial correlation functions which are just the symmetrized marginal probability density functions of K' real eigenvalues and L' complex eigenvalue pairs in the

case that the number of real eigenvalues is k' while the number of complex eigenvalues is l' with different normalizations:

$$R_{(K',L',k',l')}(\lambda_1, \dots, \lambda_{K'}, x_1 + iy_1, \dots, x_{L'} + iy_{L'}) = \frac{k'!l'!2^{l'-L'}}{(k' - K')!(l' - L')!} \int_{\mathbb{R}^{k'-K'}} \int_{\mathbb{C}_+^{2(l'-L')}} P_{N,K',L'}(\lambda_1, \dots, \lambda_{k'}, x_1 + iy_1, \dots, x_{l'} + iy_{l'}) d\lambda_{k'-K'+1} \cdots d\lambda_{k'} dx_{l'-L'+1} dy_{l'-L'+1} \cdots dx_{l'} dy_{l'}.$$

The (K', L') -correlation functions which are the symmetrized marginals of K' real eigenvalues and L' complex eigenvalue pairs with different normalization constants then decompose into a disjoint sum of probability density corresponding to having k' real and l' complex eigenvalues. They are defined as follows:

$$R_{K',L'}(\lambda_1, \dots, \lambda_{K'}, z_1, \dots, z_{L'}) = \sum_{\substack{(K',L') \\ K' \leq k', L' \leq l'}} R_{(K',L',k',l')}(\lambda_1, \dots, \lambda_{K'}, z_1, \dots, z_{L'}). \tag{31}$$

Remarkably, it is possible to express the (K', L') -correlation functions in the closed form using Pfaffians [16, 18, 20, 27]. An elegant approach to the derivation of the correlation functions is the method of skew-orthogonal polynomials [16, 18].

A family $\{q_j\}_{j=1,\dots}$ of skew-orthogonal polynomials is said to be skew-orthogonal with respect to the skew-symmetric inner product $(-, -)$, if it satisfies

$$(q_{2j}, q_{2k}) = (q_{2j+1}, q_{2k+1}) = 0 \tag{32}$$

$$(q_{2j}, q_{2k+1}) = -(q_{2j+1}, q_{2k}) = r_j \delta_{jk} \quad \text{for } j, k = 0, 1, \dots \tag{33}$$

In the context of the induced Ginibre ensemble, $(-, -)$ denotes the skew-symmetric inner product

$$\begin{aligned} (f, g) &:= (f, g)_{\mathbb{R}} + (f, g)_{\mathbb{C}} \\ (f, g)_{\mathbb{R}} &:= \int_{-\infty}^{\infty} \int_{-\infty}^{\infty} e^{-\frac{1}{2}(x^2+y^2)} \text{sgn}(y-x) |xy|^L f(x)g(y) dx dy \\ (f, g)_{\mathbb{C}} &:= 2i \int_{\mathbb{R}_+^2} e^{y^2-x^2} \text{erfc}(\sqrt{2}y) (x^2 + y^2)^L [f(x+iy)g(x-iy) - g(x+iy)f(x-iy)] dx dy. \end{aligned}$$

The method of skew-orthogonal polynomials leads to the following representation of the $(K' \cdot L')$ -correlation functions in terms of Pfaffians. A detailed derivation can be found in [18]. Denote

$$\begin{aligned} \tilde{q}(w) &:= e^{-\frac{1}{2}w^2} w^L \sqrt{\text{erfc}(\sqrt{2} \text{Im}(w))} q(w) \\ \tau_j(w) &:= \begin{cases} \frac{1}{2} \int_{\mathbb{R}} \text{sgn}(y-w) \tilde{q}_j(y) dy, & \text{if } w \in \mathbb{R} \\ i \tilde{q}_j(\bar{w}) \text{sgn}(\text{Im}(w)), & \text{if } w \in \mathbb{C} \setminus \mathbb{R} \end{cases}. \end{aligned}$$

Then,

$$R_{K',L'}(\lambda_1, \dots, \lambda_{K'}, z_1, \dots, z_{L'}) = \text{Pfaff} \begin{bmatrix} K_N(\lambda_j, \lambda_{j'}) & K_N(\lambda_j, z_{m'}) \\ K_N(z_m, \lambda_{j'}) & K_N(z_m, z_{m'}) \end{bmatrix} \tag{34}$$

with the 2×2 matrix kernel

$$K_N(w, w') := \begin{bmatrix} DS_N(w, w') & S_N(w, w') \\ -S_N(w, w') & IS_N(w, w') + \varepsilon(w, w') \end{bmatrix}, \tag{35}$$

where

$$\begin{aligned}
 DS_N(w, w') &= 2 \sum_{j=0}^{\frac{N}{2}-1} \frac{1}{r_j} [\tilde{q}_{2j}(w)\tilde{q}_{2j+1}(w') - \tilde{q}_{2j+1}(w)\tilde{q}_{2j}(w')] \\
 S_N(w, w') &= 2 \sum_{j=0}^{\frac{N}{2}-1} \frac{1}{r_j} [\tilde{q}_{2j}(w)\tau_{2j+1}(w') - \tilde{q}_{2j+1}(w)\tau_{2j}(w')] \\
 IS_N(w, w') &= 2 \sum_{j=0}^{\frac{N}{2}-1} \frac{1}{r_j} [\tau_{2j}(w)\tau_{2j+1}(w') - \tau_{2j+1}(w)\tau_{2j}(w')] \\
 \varepsilon(w, w') &= \begin{cases} \frac{1}{2} \operatorname{sgn}(w - w'), & \text{if } w, w' \in \mathbb{R} \\ 0, & \text{else} \end{cases} .
 \end{aligned}$$

The indices j and j' in (34) run from 1 to K' whilst m and m' run from 1 to L' , so that the matrix inside the Pfaffian has the block structure with the top left and right bottom blocks being of size $2K' \times 2K'$ and $2L' \times 2L'$, respectively.

The entries of the Pfaffian kernel depend on the family of polynomials q_j which are skew-orthogonal with respect to the inner product $(-, -)$. The direct computation of these polynomials is a tremendous task. As a result, a different approach is employed in order to determine the required skew-orthogonal polynomials and thus the kernel entries in (35).

As already observed in [19, 49] for the real Ginibre ensemble, the following relationship for the entry DS of the Pfaffian kernel in (35) holds true:

$$\begin{aligned}
 2 \sum_{j=0}^{\frac{N}{2}-1} \frac{1}{r_j} [q_{2j}(w)q_{2j+1}(w') - q_{2j+1}(w)q_{2j}(w')] \\
 = \frac{1}{r_N} (w - w') \langle \det(G - wI) \det(G - w'I) \rangle_{N-2}, \tag{36}
 \end{aligned}$$

where $\langle \dots \rangle_{N-2}$ denotes the average over the induced Ginibre ensemble of square matrices G of size $N - 2$, and r_N is the normalization of the N th skew-orthogonal polynomial as defined in (32).

On integrating out the ‘angular’ part of G in (36), one is left with the integral over the ‘radial’ part of G ; see e.g. [50]:

$$\langle \det(G - wI) \det(G - w'I) \rangle_{N-2} = \sum_{j=0}^{N-2} \frac{\langle \epsilon_j(GG^T) \rangle_{N-2}}{\binom{n}{j}} (ww')^{N-2-j}.$$

Here $\epsilon_j(GG^T)$ denotes the j th elementary symmetric polynomial in the eigenvalues of GG^T . The above relation can also be obtained by expanding the product of determinants on the left-hand side in Schur polynomials in the eigenvalues of G and then averaging over the orthogonal group (which is the angular part of G); see [51] for a similar integral over the unitary group.

The average $\langle \epsilon_j(GG^T) \rangle_{N-2}$ can be reduced to a Selberg–Aomoto integral [28]. As a result,

$$\begin{aligned}
 2 \sum_{j=0}^{\frac{N}{2}-1} \frac{1}{r_j} [q_{2j}(w)q_{2j+1}(w') - q_{2j+1}(w)q_{2j}(w')] \\
 = \frac{1}{r_N} (w - w') \frac{\Gamma(L + N - 1)}{\sqrt{2\pi}} \sum_{j=0}^{N-2} \frac{(ww')^j}{\Gamma(L + j + 1)}. \tag{37}
 \end{aligned}$$

As already observed in [52], the skew-orthogonal polynomials can now be just ‘read off’ using the fact that each q_j is monic and of degree j by, for example, differentiating

$$q_{2j}(w) = r_j \frac{1}{(2j+1)!} \frac{\partial^{2j+1}}{\partial u^{2j+1}} \left[\frac{1}{r_N} (u-w)\Gamma(L+N-1) \sum_{j=0}^{2j} \frac{(wu)^j}{\Gamma(L+j+1)} \right] \Bigg|_{u=0}$$

$$q_{2j+1}(w) = r_j \frac{1}{(2j)!} \frac{\partial^{2j}}{\partial u^{2j}} \left[\frac{1}{r_N} (w-u)\Gamma(L+N-1) \sum_{j=0}^{2j} \frac{(wu)^j}{\Gamma(L+j+1)} \right] \Bigg|_{u=0}.$$

Hence, for $j = 1, 2, \dots$, the following polynomials were found to be skew-orthogonal with respect to the skew-inner product $(-, -)$:

$$q_{2j}(w) = w^{2j} \quad q_{2j+1}(w) = w^{2j+1} - (2j+L)w^{2j-1}.$$

In addition to that, the first two skew-orthogonal polynomials are given by $q_0(w) = 1$ and $q_1(w) = w$. Similarly the normalization constant can be found by comparison:

$$(q_{2j}, q_{2j+1}) = 2\sqrt{2\pi}\Gamma(L+2j+1).$$

Thus, the entries of the Pfaffian kernel can be explicitly determined. A detailed derivation of the necessary computation can be found in appendix B. Here, we just state the final result in theorem 4.1 below.

Let

$$\psi(z) = e^{-\frac{1}{2}z^2} \sqrt{\operatorname{erfc}(\sqrt{2} \operatorname{Im}(z))}$$

$$t(x, z) = \frac{1}{\sqrt{2\pi}} \psi(z) 2^{\frac{L}{2}-1} z^L \frac{\Gamma(\frac{L}{2}, \frac{1}{2}x^2)}{\Gamma(L)}, \tag{38}$$

where $\Gamma(a, z)$ is the upper incomplete Gamma function

$$\Gamma(a, z) = \int_z^\infty t^{a-1} e^{-t} dt$$

and

$$s_N(z, w) = \frac{1}{\sqrt{2\pi}} \psi(z) \psi(w) \sum_{j=0}^{N-2} \frac{(wz)^{j+L}}{\Gamma(L+j+1)}$$

$$r_N(x, z) = \frac{1}{\sqrt{2\pi}} \psi(z) \operatorname{sgn}(x) 2^{\frac{N}{2}+\frac{L}{2}-\frac{3}{2}} z^{N+L-1} \frac{\gamma(\frac{N}{2} + \frac{L}{2} - \frac{1}{2}, \frac{1}{2}x^2)}{\Gamma(N+L-1)}. \tag{39}$$

Note that $s_N(z, w)$ is symmetric in its variables and $t(x, z)$ and $r_N(x, z)$ are not.

Theorem 4.1. *The entries of the complex/complex (2×2) matrix kernel $K_N(z, w)$ in (34)–(35) are given by*

$$DS_N(z, w) = (w-z)s_N(z, w); \quad S_N(z, w) = i(\bar{w}-z)s_N(z, \bar{w}); \quad IS_N(z, w) = (\bar{z}-\bar{w})s_N(\bar{z}, \bar{w}).$$

The entries of the real/complex and complex/real matrix kernels $K_N(x, z)$ and $K_N(z, x)$ in (34)–(35) are given by

$$DS_N(x, z) = (z-x)s_N(x, z); \quad DS_N(z, x) = -DS_N(x, z);$$

$$S_N(x, z) = i(\bar{z}-x)s_N(x, \bar{z}); \quad S_N(z, x) = s_N(x, z) + r_N(x, z) + t(x, z);$$

$$IS_N(x, z) = -is_N(x, \bar{z}) - ir_N(x, \bar{z}) - it(x, \bar{z}); \quad IS_N(z, x) = -IS_N(x, z).$$

And finally, the entries of the real/real matrix kernel $K_N(x, y)$ in (34)–(35) are given by

$$\begin{aligned}
 DS_N(x, y) &= (y - x)s_N(x, y); \quad S_N(x, y) = s_N(x, y) + r_N(y, x) + t(x, y); \\
 IS_N(x, y) &= \frac{1}{\sqrt{2\pi}} \left[-\frac{\gamma(L, y^2)}{\Gamma(L)} + e^{-\frac{1}{2}(x-y)^2} \frac{\gamma(L, xy)}{\Gamma(L)} + \frac{y^L e^{\frac{1}{2}y^2}}{\Gamma(L)} \int_x^y e^{-\frac{1}{2}t^2} t^{L-1} dt \right. \\
 &\quad + \frac{\gamma(L + N - 1, y^2)}{L + N - 1} - e^{-\frac{1}{2}(x-y)^2} \frac{\gamma(L + N - 1, xy)}{\Gamma(L + N - 1)} \\
 &\quad - \frac{y^{L+N-1} e^{\frac{1}{2}y^2}}{\Gamma(L + N - 1)} \int_x^y e^{-\frac{1}{2}t^2} t^{L+N-2} dt - \operatorname{sgn}(y) 2^{\frac{L}{2}+N-\frac{3}{2}} \frac{\gamma(\frac{L}{2} + \frac{N}{2} - \frac{1}{2}, \frac{1}{2}y^2)}{\Gamma(L + N - 1)} \\
 &\quad \left. \times \int_x^y e^{-\frac{1}{2}t^2} t^{L+N-1} dt - 2^{\frac{L}{2}-1} \frac{\Gamma(\frac{L}{2}, \frac{1}{2}y^2)}{\Gamma(L)} \int_x^y e^{-\frac{1}{2}t^2} t^L dt \right].
 \end{aligned}$$

4.3. Real and complex eigenvalue densities

The eigenvalue densities for finite matrix dimensions N can be read from the (K', L') -correlation functions (35) specializing to the $(0, 1)$ and $(1, 0)$ cases. Indeed,

$$\rho_N^C(z) := R_{0,1}(-, z) = \operatorname{Pfaff} K_N(z, z) = S_N(z, z) \quad (z \in \mathbb{C}_+) \tag{40}$$

is the mean density of complex eigenvalues whilst

$$\rho_N^R(x) := R_{1,0}(x, -) = \operatorname{Pfaff} K_N(x, x) = S_N(x, x) \quad (x \in \mathbb{R}) \tag{41}$$

is the mean density of real eigenvalues. Note the normalization

$$2 \int_{\mathbb{C}_+} \rho_N^C(z) d^2z + \int_{\mathbb{R}} \rho_N^R(x) dx = N.$$

Theorem 4.1 now yields the finite- N complex and real eigenvalue densities in a closed form:

$$\rho_N^C(x + iy) = \sqrt{\frac{2}{\pi}} y \operatorname{erfc}(\sqrt{2}y) e^{y^2-x^2} \sum_{j=0}^{N-2} \frac{(x^2 + y^2)^{j+L}}{\Gamma(j + L + 1)} \tag{42}$$

$$= \sqrt{\frac{2}{\pi}} y \operatorname{erfc}(\sqrt{2}y) e^{2y^2} \left[\frac{\gamma(L, x^2 + y^2)}{\Gamma(L)} - \frac{\gamma(L + N - 1, x^2 + y^2)}{\Gamma(L + N - 1)} \right], \tag{43}$$

and

$$\rho_N^R(x) = \frac{1}{\sqrt{2\pi}} e^{-x^2} \sum_{j=0}^{N-2} \frac{x^{2(j+L)}}{\Gamma(j + L + 1)} + t(x, x) + r_N(x, x) \tag{44}$$

$$= \frac{1}{\sqrt{2\pi}} \left[\frac{\gamma(L, x^2)}{\Gamma(L)} - \frac{\gamma(L + N - 1, x^2)}{\Gamma(L + N - 1)} \right] + t(x, x) + r_N(x, x), \tag{45}$$

where $t(x, x)$ and $r_n(x, x)$ are the functions defined in (38)–(39).

4.4. Asymptotic analysis

In this section, we will investigate the real induced Ginibre ensemble in the scaling limit when the free parameter L grows proportionally with the matrix dimension N , which, in the language of quadratization of rectangular matrices, corresponds to tall rectangular matrices which are neither skinny nor almost square.

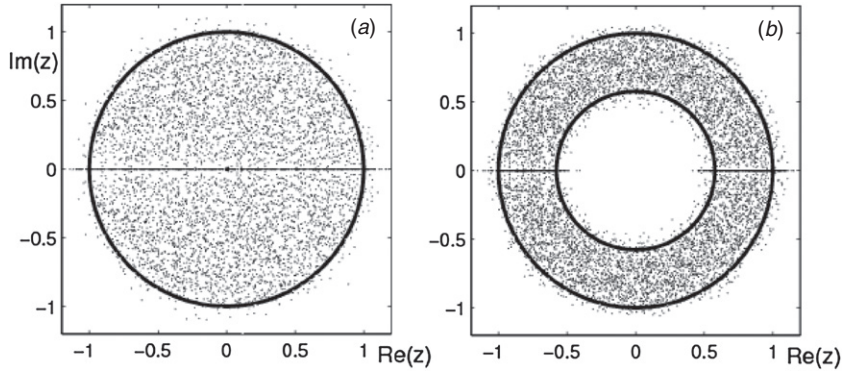


Figure 2. Spectra of random matrices from the real induced Ginibre ensemble for $N = 128$ and (a) $M = N = 128$ (no hole) and (b) $M = N + 32$. Each picture consists of 128 independent realizations and the spectra are rescaled by a factor $1/\sqrt{M}$ as in figure 1. In analogy to GinOE, we recognize a non-trivial fraction of real eigenvalues.

The real and complex eigenvalue densities $\rho_N^C(z)$ (43) and $\rho_N^R(x)$ (45) are already in a convenient form for the asymptotic analysis. The well-known limit relation for the error function [46]

$$\lim_{N \rightarrow \infty} \sqrt{N}w e^{2Nw^2} \operatorname{erfc}(\sqrt{2N}w) = \frac{1}{\sqrt{2\pi}}$$

combined with the saddle-point analysis of the integral in (23) quickly gives the limiting (mean) density of complex eigenvalues. In the leading order, the distribution of complex eigenvalues turns out to be uniform in an annulus with the inner and outer radii $r_{\text{in}} = \sqrt{L}$ and $r_{\text{out}} = \sqrt{L + N}$, exactly as in the complex induced Ginibre ensemble.

Similarly, the saddle-point analysis of each of the incomplete Gamma functions in (45) yields the limiting density of real eigenvalues. In the leading order, the real eigenvalues in the induced Ginibre ensemble populate two symmetric segments of the real axis, $[r_{\text{in}}, r_{\text{out}}]$ and $[-r_{\text{out}}, -r_{\text{in}}]$, with constant density. The theorem below summarizes our findings and figures 2 and 3 provide a comparison of the analytic results versus numerical simulations.

Theorem 4.2. *Suppose that $L = N\alpha$ with $\alpha > 0$. Then,*

- (a) *in the leading order as $N \rightarrow \infty$, the average number of real eigenvalues in the real induced Ginibre ensemble is $\sqrt{\frac{2}{\pi}}(\sqrt{L+N} - \sqrt{L})$ and the density of real eigenvalues obeys the following limiting relation:*

$$\lim_{N \rightarrow \infty} \rho_N^R(\sqrt{N}x) = \frac{1}{\sqrt{2\pi}} [\Theta(|x| - \sqrt{\alpha}) - \Theta(|x| - \sqrt{\alpha + 1})].$$

- (b) *The density of complex eigenvalues obeys the following limiting relation:*

$$\lim_{N \rightarrow \infty} \rho_N^C(\sqrt{N}z) = \frac{1}{\pi} [\Theta(|z| - \sqrt{\alpha}) - \Theta(|z| - \sqrt{\alpha + 1})].$$

On setting $L = 0$ in the above results, one recovers the expected number $\sqrt{2N/\pi}$ of real eigenvalues in the Ginibre ensemble [53] together with the uniform densities of distribution of real and complex eigenvalues [14, 53].

One can examine how quickly the eigenvalue density falls to zero when one moves away from the boundary of the eigenvalue support. At the inner and outer circular edges away from the real line, one recovers the same eigenvalue density profile as for the complex Ginibre ensemble [47].

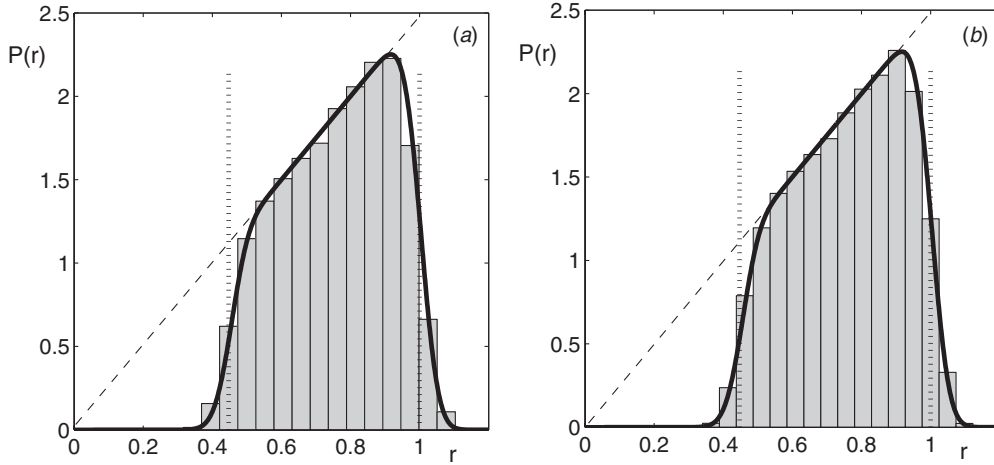


Figure 3. Radial density of complex eigenvalues of 256 realizations of (a) complex and (b) real induced Ginibre matrices of dimension $N = 128$ with $L = 32$ compared with the analytical results (solid lines) obtained from equation (22) and (43), respectively. The linear character of the curves between the inner radius, $r_{in} = \sqrt{L}/\sqrt{L+N} \approx 0.447$, and the outer radius, $r_{out} = 1$ (both rescaled by $1/\sqrt{L+N}$ and represented by vertical lines), suggests that the distribution of eigenvalues on the ring is uniform in both cases. Since the dimension N is relatively small, the area on which $P(z)$ is linear does not cover the entire interval $[r_{in}, r_{out}]$.

Theorem 4.3. Suppose that $L = N\alpha$ with $\alpha > 0$. Then, for fixed $\xi \in \mathbb{R}$ and $\phi \neq 0, \pi$:

$$\lim_{N \rightarrow \infty} \rho_N^C((\sqrt{L} - \xi) e^{i\phi}) = \lim_{N \rightarrow \infty} \rho_N^C((\sqrt{L+N} + \xi) e^{i\phi}) = \frac{1}{2\pi} \operatorname{erfc}(\sqrt{2}\xi). \tag{46}$$

It follows from (46) that the density of complex eigenvalues in the real induced Ginibre ensemble falls to zero very fast (at a Gaussian rate) away from the boundary of the eigenvalue support. This is also true of the density of real eigenvalues

Theorem 4.4. Suppose that $L = N\alpha$ with $\alpha > 0$. Then, for fixed $\xi \in \mathbb{R}$,

$$\lim_{N \rightarrow \infty} \rho_N^R(\sqrt{L} - \xi) = \lim_{N \rightarrow \infty} \rho_N^R(\sqrt{L+N} + \xi) = \frac{1}{\sqrt{2\pi}} \left[\operatorname{erfc}(\sqrt{2}\xi) + \frac{1}{2\sqrt{2}} e^{-\xi^2} \operatorname{erfc}(-\xi) \right].$$

The proofs of theorems 4.2, 4.3 and 4.4 are straightforward but tedious and are omitted.

Another interesting transitional region appears close to the real line. Here the density of complex eigenvalues is more sparse: for finite matrix dimensions $\rho_N^C(x + iy) \propto y$ for small values of y . One can easily obtain the complex eigenvalue density profile in the crossover from zero density on the real axis to the plateau of constant density far away from the real axis. For example, at the origin $\lim_{N \rightarrow \infty} \rho_N^C(iv) = \sqrt{\frac{2}{\pi}} v \operatorname{erfc}(\sqrt{2}v) e^{2v^2}$, and more generally

$$\lim_{N \rightarrow \infty} \rho_N^C(\sqrt{N}u + iv) = \sqrt{\frac{2}{\pi}} v \operatorname{erfc}(\sqrt{2}v) e^{2v^2} \quad \text{for } |u| \in (\sqrt{\alpha}, \sqrt{\alpha+1}).$$

It should be noted that apart from the support of the eigenvalue distribution which clearly depends on α , the limiting eigenvalue density profiles in various scaling regimes in the induced Ginibre ensemble are independent of α and coincide with those for the original Ginibre ensemble. This correspondence also extends to the eigenvalue correlation functions. We show in appendix D that the eigenvalue correlation functions in the induced Ginibre ensemble in the bulk and at the edges are given by the expressions obtained for the Ginibre ensemble [18]; see also [16, 17, 19].

4.5. Almost square matrices

Another interesting regime arises when the rectangularity index L is fixed instead of growing proportionally with the matrix size as discussed towards the end of section 3. In the bulk, i.e. at a distance of order \sqrt{N} from the origin, one recovers the uniform distribution of eigenvalues (real and complex) and Ginibre correlations, whereas in the vicinity of the origin, new eigenvalue statistics arise. The eigenvalue densities can be obtained by extending the summation in (42) and (44) to infinity. This yields

$$\lim_{N \rightarrow \infty} \rho_N^C(x + iy) = \sqrt{\frac{2}{\pi}} y \operatorname{erfc}(\sqrt{2}y) e^{2y^2} \frac{\gamma(L, x^2 + y^2)}{\Gamma(L)}$$

for the density of complex eigenvalues and

$$\lim_{N \rightarrow \infty} \rho_N^R(x) = \frac{1}{\sqrt{2\pi}} \left[\frac{\gamma(L, x^2)}{\Gamma(L)} + e^{-\frac{1}{2}x^2} x^L 2^{\frac{L}{2}-1} \frac{\Gamma\left(\frac{L}{2}, \frac{1}{2}x^2\right)}{\Gamma(L)} \right]$$

for the density of real eigenvalues.

As in the case of complex matrices, the higher order correlation functions at the origin are non-universal.

- (i) The limiting real/real kernel is given by a 2×2 matrix

$$K_{\text{origin}}(r, r') = \frac{1}{\sqrt{2\pi}} \begin{bmatrix} (r' - r) e^{-\frac{1}{2}(r-r')^2} \frac{\gamma(L, rr')}{\Gamma(L)} & e^{-\frac{1}{2}(r-r')^2} \frac{\gamma(L, rr')}{\Gamma(L)} + t(r, r') \\ -e^{-\frac{1}{2}(r-r')^2} \frac{\gamma(L, rr')}{\Gamma(L)} & -t(r, r') \end{bmatrix},$$

where

$$(*) = -\frac{\gamma(L, r^2)}{\Gamma(L)} + e^{-\frac{1}{2}(r-r')^2} \frac{\gamma(L, rr')}{\Gamma(L)} + \left(\frac{r^L e^{\frac{1}{2}r^2}}{\Gamma(L)} - 2^{\frac{L}{2}-1} \frac{\Gamma\left(\frac{L}{2}, \frac{1}{2}r^2\right)}{\Gamma\left(\frac{L}{2}\right)} \right) \int_x^y e^{\frac{1}{2}t^L} dt.$$

- (ii) The limiting complex/complex kernel is given by a 2×2 matrix

$$K_{\text{origin}}(z, z') = \frac{1}{\sqrt{2\pi}} \sqrt{\operatorname{erfc}(\sqrt{2} \operatorname{Im}(z)) \operatorname{erfc}(\sqrt{2} \operatorname{Im}(z'))} \\ \times \begin{bmatrix} (z - z') e^{-\frac{1}{2}(z-z')^2} \frac{\gamma(L, zz')}{\Gamma(L)} & i(\bar{z} - z') e^{-\frac{1}{2}(\bar{z}-z')^2} \frac{\gamma(L, \bar{z}z')}{\Gamma(L)} \\ i(z' - \bar{z}) e^{-\frac{1}{2}(z'-\bar{z})^2} \frac{\gamma(L, zz')}{\Gamma(L)} & (\bar{z} - \bar{z}') e^{-\frac{1}{2}(\bar{z}-\bar{z}')^2} \frac{\gamma(L, \bar{z}z')}{\Gamma(L)} \end{bmatrix}.$$

- (iii) The limiting real/complex kernel is given by a 2×2 matrix

$$K_{\text{origin}}(r, z) = \frac{1}{\sqrt{2\pi}} \sqrt{\operatorname{erfc}(\sqrt{2} \operatorname{Im}(z))} \\ \times \begin{bmatrix} (z - r) e^{-\frac{1}{2}(r-z)^2} \frac{\gamma(L, rz)}{\Gamma(L)} & i(\bar{z} - r) e^{-\frac{1}{2}(r-\bar{z})^2} \frac{\gamma(L, r\bar{z})}{\Gamma(L)} \\ -e^{-\frac{1}{2}(r-z)^2} \frac{\gamma(L, r\bar{z})}{\Gamma(L)} & -ie^{-\frac{1}{2}(r-\bar{z})^2} \frac{\gamma(L, r\bar{z})}{\Gamma(L)} - it(r, \bar{z}) \end{bmatrix}.$$

Nevertheless setting the reference points at a distance of \sqrt{N} away from the origin then yields the universal Ginibre correlation functions as given in Appendix D.

5. Quantum operations and spectra of associated evolution operators

We start this section with a brief review of quantum maps which act on the set of density operators. Later on we identify a class of maps for which the associated one-step evolution operator is represented by a rectangular real matrix. We argue that for a generic random map from this class, such an operator may be described by the induced Ginibre ensemble of real matrices.

5.1. Quantum maps

A quantum state acting on a d -dimensional Hilbert space \mathcal{H}_d can be represented by a density matrix ρ of size d . It is a positive Hermitian matrix, $\rho^\dagger = \rho \geq 0$, normalized by the trace condition, $\text{tr}\rho = 1$. Let \mathcal{M}_d denote the set of all density matrices of size d .

Consider a linear quantum map Φ , which maps the set of density matrices onto itself, $\Phi : \mathcal{M}_d \rightarrow \mathcal{M}_d$. Such a map is called *positive* as it transforms a positive operator into a positive operator. In quantum theory, one also uses a stronger property: a map is called *completely positive* if any extended map, $\Phi \otimes \mathbb{1}_n$, is positive for an arbitrary dimension n of the auxiliary subsystem.

Any completely positive map Φ can be written in the following Kraus form:

$$\rho' = \Phi(\rho) = \sum_{i=1}^k E_i \rho E_i^\dagger. \tag{47}$$

The Kraus operators $\{E_i\}_{i=1}^k$ and their number k can be arbitrary—see e.g. [54]. The map (47) preserves the trace, $\text{tr}\rho' = \text{tr}\rho$, if the entire set of k Kraus operators satisfies the identity resolution

$$\sum_{i=1}^k E_i^\dagger E_i = \mathbb{1}. \tag{48}$$

Any physical transformation of a quantum state ρ can be described by a completely positive, trace preserving map, which is also called a *quantum operation*.

Alternatively, any quantum operation can be written as a result of a unitary operation acting on an extended system and followed by the partial trace over the auxiliary subsystem E :

$$\rho' = \Phi(\rho) = \text{tr}_E[U(\rho \otimes |v\rangle\langle v|)U^\dagger]. \tag{49}$$

Here a unitary operator $U \in U(kd)$ acts on a composite Hilbert space $\mathcal{H}_S \otimes \mathcal{H}_E$, where S denotes the principal system of size d , while E denotes an environment of size k . It is assumed that the environment is described initially by a pure state $|v\rangle \in \mathcal{H}_E$.

The action of the linear transformation (47) can be described by a matrix Φ of size d^2 :

$$\rho' = \Phi\rho \quad \text{or} \quad \rho'_{m\mu} = \Phi_{m\nu}^{\mu\nu} \rho_{nv}, \tag{50}$$

where the summation over repeated indices goes from 1 to d . Since the matrices ρ and ρ' represent quantum states, so that they are positive and normalized, the matrix with exchanged indices $D_{mn} := \Phi_{m\nu}^{\mu\nu}$ is also Hermitian, positive and normalized, $\text{tr}D = d$. Thus, this matrix of rank k , called the *dynamical matrix*, is related to a quantum state ζ acting on the composed Hilbert space $\mathcal{H}_d \otimes \mathcal{H}_d$. The state ζ , proportional to the dynamical matrix, can be expressed by an extended map [54]

$$\zeta = \frac{1}{d}D = (\Phi \otimes \mathbb{1})|\psi^+\rangle\langle\psi^+|, \tag{51}$$

where $|\psi^+\rangle$ denotes the maximally entangled state, $|\psi^+\rangle = \frac{1}{\sqrt{d}} \sum_{i=1}^d |i\rangle \otimes |i\rangle$.

The dynamical matrix D is Hermitian by construction, while the superoperator matrix Φ is in general not Hermitian. The positivity of the map and the trace-preserving condition imply that the spectrum of Φ is contained in the unit disc and there exists at least one eigenvalue equal to unity. It corresponds to the invariant state of the map. The dynamical properties of the map can be described by the modulus of the subleading eigenvalue, which determines the behaviour of the system under consecutive actions of the map.

For a generic random map, distributed according to the flat (Euclidean) measure in the space of quantum operations, the subleading eigenvalue is almost surely strongly smaller than 1, which implies that the convergence to equilibrium occurs exponentially fast. In fact, statistical properties of the evolution matrix Φ of a random operation can be described by the real Ginibre ensemble [55]. The same is true for operations corresponding to quantum dynamical systems under the assumption of classical chaos and strong decoherence [9, 56]. The real ensemble is applicable here since the map Φ preserves Hermiticity and the matrix Φ becomes real in the generalized Bloch vector representation [54].

Observe that independently of the dimension k of the environment, the dimension d of the output state ρ' does not change under the action of the transformation (49), so that $\Phi : \mathcal{M}_d \rightarrow \mathcal{M}_d$. However, in several applications one uses a more general class of quantum maps, which may change the dimension of the state. Among them, one distinguishes an important class of *complementary maps*. A map $\tilde{\Phi}$ complementary to Φ can be defined as [57, 58]

$$\sigma = \tilde{\Phi}(\rho) = \text{tr}_S[U(\rho \otimes |\nu\rangle\langle\nu|)U^\dagger]. \tag{52}$$

Note that the only difference with respect to (49) is that the partial trace is performed with respect to the principal system S . The output state $\sigma \in \mathcal{M}_k$ thus describes the final state of the environment after the interaction with the system described by the global unitary matrix U . Thus, the complementary map sends the density matrix of size d into a state of size k , $\tilde{\Phi} : \mathcal{M}_d \rightarrow \mathcal{M}_k$. Comparing both maps, we see that the role of parameters d and k is interchanged: the rank of the dynamical matrix corresponding to Φ is equal to k , while for the complementary map $\tilde{\Phi}$, it is equal to d .

The complementary map $\tilde{\Phi}$ can also be described in the form (50). However, as the dimension d of the input state ρ and the dimension k of the output state σ do differ, the matrix Φ_c representing the evolution operator $\tilde{\Phi}$ under the action of a complementary map is a rectangular matrix of size $k^2 \times d^2$. To study the spectral properties of such evolution operators, one therefore has to go beyond the standard diagonalization procedure which holds for square matrices only.

5.2. Complementary maps and real induced Ginibre ensemble

We are now in a position to investigate spectral properties of evolution operators associated with a random complementary map defined by (52). As such an operator is represented by a rectangular matrix, we use formula (7) to obtain a square matrix, which can be diagonalized in the standard way.

Random complementary maps were generated numerically by selecting a fixed initial state $|\nu\rangle$ of the k dimensional environment and by plugging into (52) a random unitary matrix U distributed according to the Haar measure on $U(kd)$. This procedure allows one to generate random maps according to the Euclidean measure in the space of all quantum operations [55].

Figure 4 shows the exemplary spectra of $\tilde{\Phi}$ associated with random complementary maps, which transform an initial quantum state of size $d = 14$ into an output state of various dimensionalities. In the symmetric case $k = d$, the evolution operator is represented by a square matrix, so the spectrum covers the entire disc. In the cases $k \neq d$, the evolution operator $\tilde{\Phi}$ is represented by a rectangular matrix Φ_c . Thus, the spectrum of its quadratization $\tilde{\tilde{\Phi}}$, which corresponds to a matrix from the induced Ginibre ensemble, covers asymptotically a ring in the complex plane. The radius of the inner ring depends on the difference $|k - d|$.

Consider a random complementary map $\tilde{\Phi}$, which sends the set \mathcal{M}_d of d -dimensional states into \mathcal{M}_k . The evolution operator can be represented by a rectangular matrix Φ_c of size $k^2 \times d^2$. Assume first that $k \geq d$. Constraints imposed by the trace-preserving condition (48)

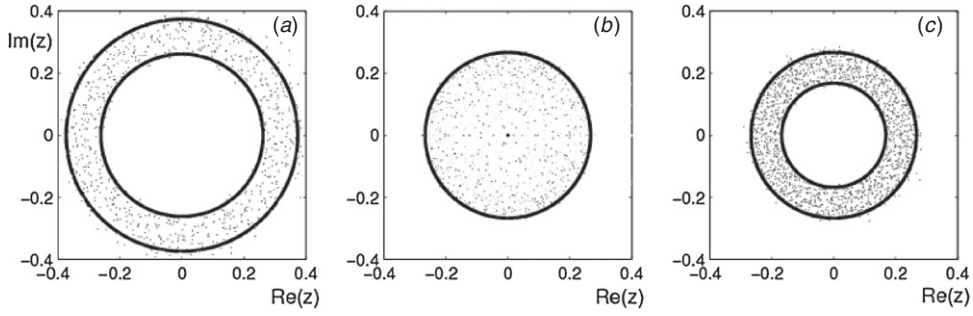


Figure 4. Spectra of operators $\tilde{\Phi}$ associated with evolution operators for generic complementary quantum maps for fixed size $d = 14$ of the initial system and different sizes of the environment (a) $k = 10$, (b) $k = 14 = d$ (which implies no hole in the support of the spectrum) and (c) $k = 18$. The data in each panel are superimposed from eight realizations of random complementary operations. Solid circles represent the radii implied by equation (54).

are known to be weak even for relatively small dimensions [9, 55], so it is legitimate to assume that Φ_c can be described by a real random rectangular matrix of the Ginibre ensemble. Thus, a quadratization $\tilde{\Phi}$ of Φ_c will be described by an appropriately rescaled matrix of the induced Ginibre ensemble with $M = k^2$ and $N = d^2$.

To find the scaling factor, we need to discuss the normalization of Φ_c . The squared norm, $\|\Phi_c\|^2 = \text{Tr}\Phi_c^\dagger\Phi_c$, is equal to the norm $\|D\|^2 = \text{Tr}D^2$ of the Hermitian dynamical matrix, which contains the same entries in a different order [54]. Since the map $\tilde{\Phi}$ changes the dimension d of the input state into k , expression (51) implies that the corresponding dynamical matrix D is a $dk \times dk$ Hermitian matrix of rank d .

Neglecting the constraints implied by the trace preserving condition, $\text{Tr}_B D = 1$, we assume that in case of a random complementary map, the dynamical matrix D behaves as a random mixed state generated by an induced measure [42]. In such a case, the average purity of a random state ρ of size N obtained from an initially random pure state of size NK by the partial trace of an over the K dimensional environment reads $\langle \text{Tr} \rho^2 \rangle = (K + N)/KN$. In the case of dynamical matrix of a complementary map, we need to substitute the correct dimensions, $N \rightarrow kd$ and $K \rightarrow d$, and use the normalization constant $D = d\zeta$ to obtain an approximate expression

$$\langle \text{Tr} D^2 \rangle = d^2 \langle \text{Tr} \zeta^2 \rangle \approx d^2 \frac{kd + d}{d^2 k} = \frac{d(k + 1)}{k} \approx d. \tag{53}$$

This in turn implies the relation $\langle \text{Tr}(\Phi_c^\dagger\Phi_c) \rangle \approx d$, so the average norm of the superoperator Φ_c representing the complementary channel $\tilde{\Phi}$ does not depend on the parameter k and can be estimated by $\|\Phi_c\| \approx \sqrt{d}$ —see figure 5.

As discussed in previous sections, an $M \times N$ matrix X (with $N \leq M$) of the Gaussian ensemble (8), for which the average norm satisfies $\langle \text{Tr} X^\dagger X \rangle = NM$, leads to a square random matrix G of size N from the induced Ginibre ensemble (13) by the way of quadratization. Its spectrum is (asymptotically) supported in the ring $r \in [r_{\text{in}}, r_{\text{out}}]$ with $r_{\text{in}} = \sqrt{L}$ and $r_{\text{out}} = \sqrt{L + N}$. To apply this ensemble for a rectangular superoperator matrix Φ_c , it is then sufficient to substitute $M \rightarrow k^2$ and $N \rightarrow d^2$ and to use the rescaling $\Phi_c = X/k\sqrt{d}$ to match the normalization. Therefore, the spectrum of the quadratization $\tilde{\Phi}$ of the superoperator Φ_c associated with the complementary map $\tilde{\Phi}$ forms a ring of the inner radius $r_{\text{in}} = \sqrt{1 - d^2/k^2}/\sqrt{d}$ while the outer radius reads $r_{\text{out}} = 1/\sqrt{d}$.

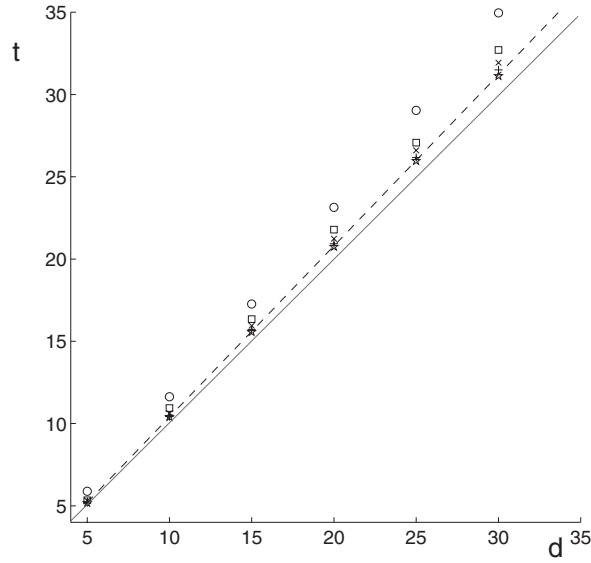


Figure 5. Average squared norm of the superoperator related to the complementary map $t = \langle \text{Tr} \Phi_c^\dagger \Phi_c \rangle$ as a function of size d of the input system. Various symbols denote different values of the size of the output system, $k = 5$ (\circ), $k = 10$ (\square), $k = 15$ (\times), $k = 20$ ($+$) and $k = 25$ (\star). The dashed line is plotted to guide the eye. It corresponds to $k = 25$ and shows that the bigger the value of k , the better the approximation to the asymptote represented by the solid diagonal line.

Consider now the other case in which the dimensions determining the complementary map satisfy $k \leq d$. Then, the superoperator Φ_c , represented by a rectangular matrix $k^2 \times d^2$, gets its quadratization by the same procedure from the transposed matrix as mentioned in section 2, and again it is described by the induced Ginibre matrices with the level density analysed in section 4. The key difference with respect to this distribution, describing the transposed rectangular matrix X^T , is that the role of variables M and N is exchanged. Hence, in the case for the transposed superoperator Φ_c^T , one needs to exchange the dimensions k and d . Taking this into account and the normalization $\|\Phi_c\|^2 \approx d$, one infers that the outer radius of the ring reads in this case $r_{\text{out}} = \sqrt{d^2/k} \sqrt{d} = \sqrt{d/k}$.

Thus, the square matrices $\tilde{\Phi}$ associated with the superoperators corresponding to random complementary maps $\tilde{\Phi} : \mathcal{M}_d \rightarrow \mathcal{M}_k$ can be described with real matrices of the induced Ginibre ensemble. Apart from the leading eigenvalue $\lambda_1 = 1$, which is implied by the trace preserving condition, the spectra are asymptotically localized in a ring in the complex plane. Both radii of the ring read

$$[r_{\text{in}}, r_{\text{out}}] = \begin{cases} \left[\frac{1}{\sqrt{d}} \sqrt{1 - \frac{d^2}{k^2}}, \frac{1}{\sqrt{d}} \right] & \text{for } k \geq d \\ \left[\frac{\sqrt{d}}{k} \sqrt{1 - \frac{k^2}{d^2}}, \frac{\sqrt{d}}{k} \right] & \text{for } k \leq d. \end{cases} \quad (54)$$

The above predictions show good agreement with numerical data obtained for several realizations of random complementary maps and shown in figure 4. To obtain a clearer figure, the plot is magnified by a factor \sqrt{d} .

6. Concluding remarks

Although the specific example of the Ginibre ensemble is completely solved, the theory of non-Hermitian random matrices is still far from being as thoroughly understood as its Hermitian counterpart. In this work, we have introduced a new generalization of the ensemble of non-Hermitian Ginibre matrices and derived explicit results for spectral density in the complex and real cases. Using the method of skew-orthogonal polynomials, we derived various spectral correlation functions which can be expressed as Pfaffians. Analysing asymptotic behaviour in the limit of large matrix dimensions, we have found a universal behaviour of the eigenvalue statistics.

The induced Ginibre ensemble of square matrices of size N is parametrized by a single discrete parameter $L \geq 0$. In the case $L = 0$, the model reduces to the standard Ginibre ensemble [1], with the eigenvalues, for large N , uniformly distributed in the disc of radius \sqrt{N} about the origin, while for $L > 0$ the eigenvalues are repelled from the origin and form a ring in the complex plane $\sqrt{L} < |z| < \sqrt{N+L}$.

This form of the spectrum suggests a comparison with the model (2) of Feinberg–Zee for which the ‘single ring’ theorem was proven [33, 35, 59]. Our model formally belongs to the Feinberg–Zee class, with the potential

$$V(G^\dagger G) = G^\dagger G - L \log G^\dagger G, \tag{55}$$

but due to the log function the assumption that the potential is polynomial is not satisfied. Analysing the joint probability distribution for the induced Ginibre ensemble, it is easy to see that eigenvalues near the origin are unlikely, which implies the ring of eigenvalues. On the other hand, it is not simple to find a specific mechanism responsible for the single ring distribution for the general version of the Feinberg–Zee model. Furthermore, in the latter model, the eigenvalue correlation functions are not known while we could compute them for the induced Ginibre ensemble for the complex and real versions of the model.

Our work leads to a straightforward explicit algorithm to generate random matrices from the induced Ginibre ensemble. It is sufficient to take a rectangular $M \times N$ random Gaussian matrix X , construct the positive Wishart-like matrix, $X^\dagger X$ of size N , take its square root and multiply it by a random unitary U distributed according to the Haar measure on the unitary group $U(N)$. The result $G = U \sqrt{X^\dagger X}$ is distributed according to the desired joint probability function (3), while its singular values are described by the Marchenko–Pastur distribution with the parameter $c = M/N$. This follows from the fact that $G^\dagger G = X^\dagger X$; hence, the square random matrix G has the same singular values as the initial rectangular Gaussian matrix X .

Alternatively, the square random matrices from the induced Ginibre ensemble can be obtained by the quadratization (5)–(7) of rectangular Gaussian matrices. Although for a given rectangular matrix various quadratization algorithms produce different square matrices, the statistical properties of square matrices obtained by quadratization of rectangular random Gaussian matrices do not depend on the choice of the algorithm.

An analogous construction also works in the real case. Take a rectangular $M \times N$ real Ginibre matrix X , construct the square root of the positive Wishart matrix $X^T X$ and multiply it by a random orthogonal matrix O distributed according to the Haar measure on the orthogonal group $O(N)$. The result $G = O \sqrt{X^T X}$ is then distributed according to the induced ensemble of real Ginibre matrices, specified by (3) with $\beta = 1$.

The induced ensemble of random Ginibre matrices offers a simple model for further research within the developing theory of non-Hermitian random matrices. We are tempted to believe that it will find its applications in several fields of physics. For instance, they can be helpful for the analysis of evolution operators associated with certain classes of generic

quantum maps. In the simplest case, as the dimension of the input and output states are the same, the associated evolution operator can be described by the standard ensemble of real Ginibre matrices [9]. However, studying complementary quantum operations, or other quantum maps in which the dimensions of the initial and the final states do differ, one copes with evolution operators represented by rectangular matrices. Our work provides evidence that the statistical properties of square matrices associated with the evolution operators for complementary quantum maps do correspond to the induced ensemble of real Ginibre matrices.

Acknowledgments

We would like to thank Gernot Akemann, Marek Bożejko, Yan Fyodorov, Dmitry Savin and the anonymous referees for their useful comments; one of the referees' comments is reproduced in the footnote following equation (6). Financial support by the SFB Transregio-12 project der Deutschen Forschungsgemeinschaft and the grant financed by the Polish National Science Centre under the contract number DEC-2011/01/M/ST2/00379 is gratefully acknowledged.

Appendix A. Proof of lemma 2.1

Assuming W as in (6), by multiplying through in (5), one obtains an equation for C , $C^\dagger Y + (\mathbb{1}_{M-N} - C^\dagger C)^{1/2} Z = 0$. Hence,

$$Z = -(\mathbb{1}_{M-N} - C^\dagger C)^{-1/2} C^\dagger Y = -C^\dagger (\mathbb{1}_N - CC^\dagger)^{-1/2} Y. \quad (\text{A.1})$$

Consequently, by making use of (5) again,

$$G = (\mathbb{1}_N - CC^\dagger)^{1/2} Y - CZ = (\mathbb{1}_N - CC^\dagger)^{-1/2} Y. \quad (\text{A.2})$$

It is easy to check that

$$Z^\dagger Z = Y^\dagger (\mathbb{1}_N - CC^\dagger)^{-1} Y - Y^\dagger Y \quad (\text{A.3})$$

which implies that

$$Y^\dagger Y + Z^\dagger Z = Y^\dagger (\mathbb{1}_N - CC^\dagger)^{-1} Y. \quad (\text{A.4})$$

This in turn allows us to write

$$(\mathbb{1}_N - CC^\dagger)^{-1} = \frac{1}{Y^\dagger} (Y^\dagger Y + Z^\dagger Z) \frac{1}{Y}, \quad (\text{A.5})$$

which when substituted into (A.2) yields (7). Note that the desired result (7) can also be rewritten in a more symmetric form

$$G = Y (Y^\dagger Y)^{-1/2} (\mathbb{1}_N + (Y^\dagger Y)^{-1/2} Z^\dagger Z (Y^\dagger Y)^{-1/2})^{1/2} (Y^\dagger Y)^{1/2}, \quad (\text{A.6})$$

which shows that all matrix square roots operate correctly on positive definite objects.

Appendix B. Proof of theorem 4.1

In this appendix, we determine the finite N correlation functions for the real induced Ginibre by determining the matrix entries of the Pfaffian kernel given in (34) and hence prove theorem 4.1. Equipped with the appropriate skew-orthogonal polynomials and their normalization, the task of determining the entries of the matrix kernel for the (j, m) -correlation functions can now proceed. Firstly (37) implies for $w, z \in \mathbb{C}$:

$$DS_N(z, w) = \frac{1}{\sqrt{2\pi}} \psi(w) \psi(z) (z - w) \sum_{j=0}^{N-2} \frac{(wz)^{j+L}}{\Gamma(L + j + 1)}. \quad (\text{B.1})$$

Noting that $S_N(z, w) = iDS_N(z, \bar{w})$ and $IS_N(z, w) = -DS_N(\bar{z}, \bar{w})$, we have completely determined the entries of the complex–complex matrix kernel.

Let us next consider the case $x \in \mathbb{R}$, $z \in \mathbb{C}$. The following approach is borrowed from [16]. We observe that

$$q_{2j+1}(x) = -e^{\frac{1}{2}x^2} x^{-L} \frac{\partial}{\partial x} \left[e^{-\frac{1}{2}x^2} x^{2j+L} \right],$$

which implies for $j > 0$

$$\tau_{2j+1}(x) = e^{-\frac{1}{2}x^2} x^{j+L}.$$

Furthermore, direct computation shows that

$$\tau_1(x) - \frac{L}{2} \int_{\mathbb{R}} \operatorname{sgn}(x-t) e^{-\frac{1}{2}t^2} x^{L-1} dt = e^{-\frac{1}{2}x^2} x^{2j+L}.$$

All in all

$$\begin{aligned} \sum_{j=0}^{\frac{N}{2}-1} \frac{1}{r_j} \tilde{q}_{2j}(z) \tau_{2j+1}(x) &= \frac{1}{\sqrt{2\pi}} \psi(z) e^{-\frac{1}{2}x^2} \sum_{j=1}^{\frac{N}{2}-1} \frac{(xz)^{L+2j}}{\Gamma(L+2j+1)} \\ &\quad + \frac{1}{\sqrt{2\pi}\Gamma(L+1)} \psi(z) z^L \left[\tau_1(x) - \frac{L}{2} \int_{\mathbb{R}} \operatorname{sgn}(x-t) e^{-\frac{1}{2}t^2} x^{L-1} dt \right] \\ &\quad + \frac{1}{\sqrt{2\pi}\Gamma(L+1)} \psi(z) z^L \frac{L}{2} \int_{\mathbb{R}} \operatorname{sgn}(x-t) e^{-\frac{1}{2}t^2} x^{L-1} dt \\ &= \frac{1}{\sqrt{2\pi}} e^{-\frac{1}{2}x^2 - \frac{1}{2}z^2} \sqrt{\operatorname{erfc}(\sqrt{2}\operatorname{Im}(z))} \sum_{j=0}^{\frac{N}{2}-1} \frac{(xz)^{L+2j}}{\Gamma(L+2j+1)} \\ &\quad + \frac{1}{\sqrt{2\pi}} \psi(z) z^L 2^{\frac{L}{2}-1} \frac{\Gamma(\frac{L}{2}, \frac{1}{2}x^2)}{\Gamma(L+1)}. \end{aligned}$$

In addition to that

$$\begin{aligned} S &= \sum_{j=0}^{\frac{N}{2}-1} \frac{1}{r_j} \tilde{q}_{2j+1}(z) \tau_{2j}(x) \\ &= \frac{1}{\sqrt{2\pi}} \psi(z) z^L \sum_{j=1}^{\frac{N}{2}-1} \frac{[z^{2j+1} - (L+2j)z^{2j-1}] \tau_{2j}(x)}{\Gamma(L+2j+1)} + \frac{1}{\sqrt{2\pi}\Gamma(L+1)} \psi(z) z^L \tau_0(x). \end{aligned}$$

Rearranging the summation gives

$$\begin{aligned} S &= \frac{1}{\sqrt{2\pi}\Gamma(L+N-1)} \psi(z) z^{L+N-1} \tau_{N-2}(x) \\ &\quad - \frac{1}{\sqrt{2\pi}} \psi(z) z^L \sum_{j=0}^{\frac{N}{2}-2} \frac{[\tau_{2j+2}(x) - (L+j+1)\tau_{2j}(x)] z^{2j+1}}{\Gamma(L+2j+1)}. \end{aligned}$$

Another differential equation

$$q_{2j+2}(x) - (2j+L+1)q_{2j}(x) = -e^{\frac{1}{2}x^2} x^{-L} \frac{\partial}{\partial x} \left[e^{-\frac{1}{2}x^2} x^{2j+L+1} \right]$$

leads to

$$\tau_{2j+2}(x) - (2j+L+1)\tau_{2j}(x) = e^{-\frac{1}{2}x^2} x^{2j+L+1}.$$

As a consequence

$$S = -\frac{1}{\sqrt{2\pi}} \psi(z) z^{L+N-1} 2^{\frac{L}{2}+N-\frac{3}{2}} \operatorname{sgn}(x) \frac{\gamma\left(\frac{L}{2} + \frac{N}{2} - \frac{1}{2}, \frac{1}{2}x^2\right)}{\Gamma(L+N-1)} - \frac{1}{\sqrt{2\pi}} \psi(z) e^{-\frac{1}{2}x^2} \sum_{j=0}^{\frac{N}{2}-2} \frac{(xz)^{L+2j+1}}{\Gamma(L+2j+2)}.$$

Finally, we obtain

$$S_N(z, w) = \frac{1}{\sqrt{2\pi}} e^{-\frac{1}{2}x^2} \psi(z) \sum_{j=0}^{N-2} \frac{(xz)^{L+2j}}{\Gamma(L+2j+1)} + \frac{1}{\sqrt{2\pi}} \psi(z) z^{L+N-1} 2^{\frac{L}{2}+N-\frac{3}{2}} \operatorname{sgn}(x) \frac{\gamma\left(\frac{L}{2} + \frac{N}{2} - \frac{1}{2}, \frac{1}{2}x^2\right)}{\Gamma(L+N-1)} + \frac{1}{\sqrt{2\pi}} \psi(z) 2^{\frac{L}{2}-1} \frac{\Gamma\left(\frac{L}{2}, \frac{1}{2}x^2\right)}{\Gamma(L+1)}.$$

The last entry requiring explicit computation is $IS_N(x, y)$ for $x, y \in \mathbb{R}$. In this case, the relationship

$$IS_N(x, y) = - \int_x^y S_N(t, y) dt$$

comes in handy. Using the expression obtained for $S_N(x, y)$ and in addition to that employing the integral representation

$$e^{-ty} \sum_{j=0}^{N-2} \frac{(ty)^{L+2j}}{\Gamma(L+2j+1)} = \left[\frac{\gamma(L, ty)}{\Gamma(L)} - \frac{\gamma(L+N-1, ty)}{\Gamma(L+N-1)} \right]$$

leads to the following starting point for our derivation

$$IS_N(x, y) = -\frac{1}{\sqrt{2\pi}\Gamma(L)} \int_x^y e^{-\frac{1}{2}(t-y)^2} (y-t) \gamma(L, ty) dt + \frac{1}{\sqrt{2\pi}\Gamma(L+N-1)} \int_x^y e^{-\frac{1}{2}(t-y)^2} (y-t) \gamma(L+N-1, ty) dt - \frac{1}{\sqrt{2\pi}} \operatorname{sgn}(x) 2^{\frac{L}{2}+N-\frac{3}{2}} \frac{\gamma\left(L + \frac{N}{2} - \frac{1}{2}, \frac{1}{2}x^2\right)}{\Gamma(L+N-1)} \int_x^y e^{\frac{1}{2}t^2} t^{L+N-1} dt - \frac{1}{\sqrt{2\pi}} \frac{\Gamma\left(\frac{L}{2}, \frac{1}{2}x^2\right)}{\Gamma(L+1)} \int_x^y e^{\frac{1}{2}t^2} t^L dt.$$

The above expression can be simplified by employing integration by parts with respect to t . As a conclusion, we have derived all the possible entries of the Pfaffian matrix kernel.

Appendix C. Asymptotic analysis of correlation functions

In this appendix, we state the asymptotic behaviour of the correlation functions of the complex induced Ginibre ensemble for different scaling regimes.

Theorem C.1 (The limiting correlation functions in the bulk). *Let u, z_1, \dots, z_n be complex numbers and set $\lambda_k = \sqrt{N}u + z_k$ for $k = 1, \dots, n$ and $L = N\alpha$; then, for $u \in R$*

$$\lim_{N \rightarrow \infty} R_n(\lambda) = \det \left[\frac{1}{\pi} \exp \left(-\frac{|z_j|}{2} - \frac{|z_k|}{2} + z_j \bar{z}_k \right) \right]_{j,k=1}^n$$

with $R = \{r \in \mathbb{C} | \sqrt{\alpha} \leq |r| \leq \sqrt{\alpha+1}\}$.

Proof. We need to analyse the asymptotics of the kernel

$$\begin{aligned}
 K_N(z_j, z_k) &= \frac{1}{\pi} e^{-\frac{1}{2} \left(|\sqrt{N}u+z_j| |\sqrt{N}\bar{u}+\bar{z}_j| - \frac{1}{2} |\sqrt{N}u+z_k| |\sqrt{N}\bar{u}+\bar{z}_k| \right)} \\
 &\quad \times \sum_{l=0}^{N-1} \frac{\left(|\sqrt{N}u+z_j| |\sqrt{N}\bar{u}+\bar{z}_k| \right)^{l+L}}{\Gamma(l+L+1)} \\
 &= \frac{1}{\pi} e^{-N|u|^2 - \sqrt{N}(u\bar{z}_k + \bar{u}z_j) - z_j\bar{z}_k} e^{-\frac{|z_j|^2}{2} - \frac{|z_k|^2}{2} + z_j\bar{z}_k} e^{\frac{\sqrt{N}}{2}(u\bar{z}_j - u\bar{z}_j)} e^{-\frac{\sqrt{N}}{2}(\bar{u}z_k - u\bar{z}_k)} \\
 &\quad \times \sum_{l=0}^{N-1} \frac{(N|u|^2 + \sqrt{N}(u\bar{z}_k + \bar{u}z_j) + z_j\bar{z}_k)^{l+L}}{\Gamma(l+L+1)}.
 \end{aligned}$$

In order to simplify this expression, we resort to the following trick outlined in [18]. We set $\psi_N(z_j) = e^{\frac{\sqrt{N}}{2}(u\bar{z}_j - u\bar{z}_j)}$ and define the diagonal matrix

$$D_n = \text{diag}(\psi_N(z_1), \psi_N(z_2), \dots, \psi_N(z_n)).$$

We note the following: $|\psi_N(s)| = 1$ and as a consequence

$$R_n(\lambda) = \det(D_n)R_n(\lambda)\det(D_n^\dagger).$$

Thus, we can write for the n -point correlation function

$$\begin{aligned}
 R_n(\lambda) &= \det \left[\frac{1}{\pi} e^{-\frac{|z_j|^2}{2} - \frac{|z_k|^2}{2} + z_j\bar{z}_k} e^{-N|u|^2 - \sqrt{N}(u\bar{z}_k + \bar{u}z_j) - z_j\bar{z}_k} \right. \\
 &\quad \left. \times \sum_{l=0}^{N-1} \frac{(N|u|^2 + \sqrt{N}(u\bar{z}_k + \bar{u}z_j) + z_j\bar{z}_k)^{l+L}}{\Gamma(l+L+1)} \right]_{j,k=1}^n.
 \end{aligned}$$

Applying another saddle-point analysis, it can be shown that for $u \in R$

$$\lim_{N \rightarrow \infty} e^{-N|u|^2 - \sqrt{N}(u\bar{z}_k + \bar{u}z_j) - z_j\bar{z}_k} \sum_{l=0}^{N-1} \frac{(N|u|^2 + \sqrt{N}(u\bar{z}_k + \bar{u}z_j) + z_j\bar{z}_k)^{l+L}}{\Gamma(l+L+1)} = 1,$$

which gives the limiting expression for the n -point correlation functions. □

Employing the same technique again, albeit with a slightly different saddle-point method, yields the limiting behaviour of the n -point correlation functions around the circular edges of the eigenvalue density.

Theorem C.2 (The limiting correlation functions at the edges). *Let u, z_1, \dots, z_n be complex numbers with $|u| = 1$.*

(1) *Setting $\lambda_k = \sqrt{N(\alpha + 1)}u + z_k$ for $k = 1, \dots, n$ leads to the limiting correlation functions at the outer edge $\sqrt{N(\alpha + 1)}$:*

$$\lim_{N \rightarrow \infty} R_n(\lambda_1, \dots, \lambda_n) = \det \left[\frac{1}{2\pi} \exp \left(-\frac{|z_j|^2}{2} - \frac{|z_k|^2}{2} + z_j\bar{z}_k \right) \left(\text{erfc} \left(\frac{z_j\bar{u} + \bar{z}_k u}{\sqrt{2}} \right) \right) \right]_{j,k=1}^n.$$

The same limiting expression is found around the inner edge $\sqrt{N\alpha}$ of the eigenvalue density by setting $\lambda_k = \sqrt{N\alpha}u - z_k$ for $k = 1, \dots, n$.

Appendix D. Limiting correlation functions for the real induced Ginibre ensemble

Throughout this section, it is assumed that $L = N\alpha$.

Theorem D.1 (The limiting correlation functions in the bulk). *Let $u \in \mathbb{R}$ such that $\sqrt{\alpha} < |u| < \sqrt{\alpha + 1}$ and let $r_1, \dots, r_j \in \mathbb{R}$ as well as $s_1, \dots, s_m \in \mathbb{C}_+ \setminus \mathbb{R}$. Furthermore, set $x_t = \sqrt{Nu} + r_t$ for $t = 1, \dots, j$, $z_v = \sqrt{Nu} + s_v$ for $v = 1, \dots, m$ and $L = N\alpha$; then,*

$$\lim_{N \rightarrow \infty} R_{j,m}(x_1, \dots, x_j, z_1, \dots, z_m) = \text{Pfaff} \begin{bmatrix} K(r_t, r_{t'}) & K(r_t, s_{v'}) \\ K(s_v, r_{t'}) & K(s_v, s_{v'}) \end{bmatrix}$$

where $t, t' = 1, \dots, j$ and $v, v' = 1, \dots, m$.

(i) The limiting real/real kernel is given by

$$K(r, r') = \begin{bmatrix} \frac{1}{\sqrt{2\pi}}(r - r') e^{-\frac{1}{2}(r-r')^2} & \frac{1}{\sqrt{2\pi}} e^{-\frac{1}{2}(r-r')^2} \\ -\frac{1}{\sqrt{2\pi}} e^{-\frac{1}{2}(r-r')^2} & \frac{1}{2} \text{sgn}(r - r') \text{erfc} \left(\frac{|r-r'|}{\sqrt{2}} \right) \end{bmatrix}.$$

(ii) The limiting complex/complex kernel is given by

$$K(z, z') = \frac{1}{\sqrt{2\pi}} \sqrt{\text{erfc}(\sqrt{2} \text{Im}(z)) \text{erfc}(\sqrt{2} \text{Im}(z'))} \\ \times \begin{bmatrix} (z' - z) e^{-\frac{1}{2}(z-z')^2} & i(\bar{z} - z') e^{-\frac{1}{2}(z-\bar{z}')^2} \\ i(z' - \bar{z}) e^{-\frac{1}{2}(\bar{z}-z')^2} & (\bar{z} - \bar{z}') e^{-\frac{1}{2}(\bar{z}-\bar{z}')^2} \end{bmatrix}.$$

(iii) The limiting real/complex kernel is given by

$$K(r, z) = \frac{1}{\sqrt{2\pi}} \sqrt{\text{erfc}(\sqrt{2} \text{Im}(z))} \begin{bmatrix} (z - r) e^{-\frac{1}{2}(r-z)^2} & i(\bar{z} - r) e^{-\frac{1}{2}(r-\bar{z})^2} \\ -e^{-\frac{1}{2}(x-z)^2} & -i e^{-\frac{1}{2}(x-\bar{z})^2} \end{bmatrix}.$$

Proof. In the following, only the derivation of the limiting behaviour of the real/real kernel will be outlined, as this is the most involved computation. All other results can be deduced in a similar fashion. We start by computing the asymptotic behaviour of S_N . Using the results from appendix C.1, it is obvious that

$$\lim_{N \rightarrow \infty} s_N(\sqrt{Nu} + r, \sqrt{Nu} + r') = \frac{1}{\sqrt{2\pi}} e^{-\frac{1}{2}(r-r')^2}.$$

The next term to be analysed is

$$r_N(\sqrt{Nu} + r, \sqrt{Nu} + r') = \frac{1}{\sqrt{2\pi}} \text{sgn}(\sqrt{Nu} + r) \frac{2^{\frac{N}{2}(\alpha+1)-\frac{3}{2}}}{\Gamma(N(\alpha+1) - 1)} \\ \times e^{-\frac{1}{2}(\sqrt{Nu}+r')^2} (\sqrt{Nu} + r')^{N(\alpha+1)-1} \gamma \left(\frac{N}{2}(\alpha+1) - \frac{1}{2}, \frac{1}{2}(\sqrt{Nu} + r^2) \right).$$

We can apply the duplication formula for the gamma function

$$\Gamma(2z) = \Gamma(z) \Gamma \left(z + \frac{1}{2} \right) 2^{2z-1} \frac{1}{\sqrt{\pi}}$$

and obtain

$$r_N(\sqrt{Nu} + r, \sqrt{Nu} + r') = \text{sgn}(\sqrt{Nu} + r) 2^{\frac{N}{2}(\alpha+1)-\frac{3}{2}} e^{-\sqrt{Nu}r'} \left(1 + \frac{r'}{\sqrt{Nu}} \right)^{N(\alpha+1)-1} \\ \times \frac{[Nu^2]^{\frac{N}{2}(\alpha+1)-\frac{1}{2}}}{\Gamma \left(\frac{N}{2}(\alpha+1) \right) \Gamma \left(\frac{N}{2}(\alpha+1 - \frac{1}{2}) \right)} \gamma \left(\frac{N}{2}(\alpha+1) - \frac{1}{2}, \frac{1}{2}(\sqrt{Nu} + r^2) \right).$$

Furthermore, the use of the Stirling formula

$$\Gamma(z) \sim e^{-x} x^x \sqrt{\frac{2\pi}{x}},$$

as well as

$$\left(1 + \frac{r'}{\sqrt{Nu}}\right)^{N(\alpha+1)-1} \sim e^{\sqrt{N}(\alpha+1)\frac{s}{u} - \frac{s^2}{2u^2}},$$

leads to

$$r_N(\sqrt{Nu} + r, \sqrt{Nu} + r') \sim \text{sgn}(u) \frac{1}{\sqrt{\pi}} e^{\sqrt{Ns}(\frac{\alpha+1-u^2}{u})} e^{-\frac{1}{2}s^2(\frac{\alpha+1+u^2}{u^2})} e^{\frac{N}{2}(\alpha+1-u^2+2(\alpha+1)\ln(\frac{u^2}{\alpha+1}))} \frac{1}{\Gamma(\frac{N}{2}(\alpha+1-\frac{1}{2}))} \gamma\left(\frac{N}{2}(\alpha+1) - \frac{1}{2}, \frac{1}{2}(\sqrt{Nu} + r^2)\right).$$

Now it can easily be seen that

$$\lim_{N \rightarrow \infty} e^{\sqrt{Ns}(\frac{\alpha+1-u^2}{u})} e^{-\frac{1}{2}s^2(\frac{\alpha+1+u^2}{u^2})} = 0.$$

In addition to that for $|u|^2 < \alpha + 1$, the expression $\alpha + 1 - u^2 + 2(\alpha + 1) \ln(\frac{u^2}{\alpha+1})$ is negative and a saddle point method shows that

$$\lim_{N \rightarrow \infty} \frac{1}{\Gamma(\frac{N}{2}(\alpha+1-\frac{1}{2}))} \gamma\left(\frac{N}{2}(\alpha+1) - \frac{1}{2}, \frac{1}{2}(\sqrt{Nu} + r^2)\right) = 0.$$

As a conclusion, we have shown that $\lim_{N \rightarrow \infty} r_N(\sqrt{Nu} + r, \sqrt{Nu} + r') = 0$. The next term

$$t(\sqrt{Nu} + r, \sqrt{Nu} + r') = \frac{1}{\sqrt{2\pi}} \frac{2^{\frac{N\alpha}{2}-1}}{\Gamma(N\alpha)} e^{-\frac{1}{2}(\sqrt{Nu}+r')^2} (\sqrt{Nu} + r')^{N\alpha} \Gamma\left(\frac{N}{2}\alpha, \frac{1}{2}(\sqrt{Nu} + r^2)\right)$$

can be dealt with in a similar fashion. We have now determined the scaling limits of the real/real entries S_N and DS_N . The scaling limit for the entry IS_N can be found by applying a saddle point method on each of the eight integrals. In addition to that the asymptotic relationships derived for r_N and t can be applied. □

Similar calculations lead to the conclusion that in the complex bulk and also at the edges the eigenvalue correlation functions in the real induced Ginibre are exactly the same as those in the real Ginibre ensemble. We omit the derivations and only state the results in the two theorems below.

Theorem D.2 (The limiting correlation functions in the complex bulk). *Let u be a complex number such that $u \in R = \{r \in \mathbb{C} | \sqrt{\alpha} \leq |r| \leq \sqrt{\alpha+1}\}$ and let $s_1, \dots, s_m \in \mathbb{C}$. Furthermore, set $z_j = \sqrt{Nu} + s_j$ for $j = 1, \dots, m$ and $L = N\alpha$; then, for $u \in R$*

$$\lim_{N \rightarrow \infty} R_{0,m}(-, z_1, \dots, z_m) = \frac{1}{\pi} \det \left[\exp\left(-\frac{|s_k|}{2} - \frac{|s_{k'}|}{2} + z_k \bar{z}_{k'}\right) \right]_{k,k'=1,\dots,m}.$$

Theorem D.3 (The limiting correlation functions at the edges). *Let $u = \pm 1, r_1, \dots, r_l \in \mathbb{R}$ as well as $s_1, \dots, s_m \in \mathbb{C}_+$. Setting $x_j = \sqrt{N(\alpha+1)}u + r_j$ for $t = 1, \dots, l$ and $z_k = \sqrt{N(\alpha+1)}u + s_k$ for $k = 1, \dots, m$ leads to Ginibre behaviour for the limiting correlation functions at the outer edge of the eigenvalue distribution as described in [18]. In addition, at the inner circular edge $x_j = \sqrt{N\alpha}u - r_j$ for $t = 1, \dots, l$ and $z_k = \sqrt{N\alpha}u - s_k$ for $k = 1, \dots, m$, the Ginibre limiting correlation functions can again be recovered.*

References

- [1] Ginibre J 1965 Statistical ensembles of complex, quaternion, and real matrices *J. Math. Phys.* **6** 440–9
- [2] Haake F 2010 *Quantum Signatures of Chaos* 3rd edn (Berlin: Springer)
- [3] Beenakker C W J 1997 Random-matrix theory of quantum transport *Rev. Mod. Phys.* **69** 731–808
- [4] Efetov K B 1997 Quantum disordered systems with a direction *Phys. Rev. B* **56** 9630–48
- [5] Bouchaud J P and Potters M 2004 *Theory of Financial Risk and Derivative Pricing: From Statistical Physics to Risk Management* 2nd edn (Cambridge: Cambridge University Press)
- [6] Kwapien J, Drożdż S, Górski A Z and Oświęcimka P 2006 Asymmetric matrices in an analysis of financial correlations *Acta Phys. Pol. B* **37** 3039–48
- [7] Kwapien J, Drożdż S and Ioannides A A 2000 Temporal correlations versus noise in the correlation matrix formalism: an example of the brain auditory response *Phys. Rev. E* **62** 5557–64
- [8] Šeba P 2003 Random matrix analysis of human EEG data *Phys. Rev. Lett.* **91** 198104
- [9] Bruzda W, Smaczynski M, Cappellini V, Sommers H-J and Życzkowski K 2010 Universality of spectra for interacting quantum chaotic systems *Phys. Rev. E* **81** 066209
- [10] Tulino A M and Verdu S 2004 *Random Matrix Theory and Wireless Communications* (Hannover, MA: Now Publishers Inc.)
- [11] Timme M, Wolf F and Geisel T 2002 Coexistence of regular and irregular dynamics in complex networks of pulse-coupled oscillators *Phys. Rev. Lett.* **89** 258701
- [12] Sinclair C D 2007 Averages over Ginibre’s ensemble of random real matrices *Int. Math. Res. Not.* **2007** rnm015
- [13] Lehmann N and Sommers H-J 1991 Eigenvalue statistics of random real matrices *Phys. Rev. Lett.* **67** 941–4
- [14] Edelman A 1997 The probability that a random real Gaussian matrix has k real eigenvalues, related distributions, and the circular law *J. Multivariate Anal.* **60** 203–32
- [15] Akemann G and Kanzieper E 2007 Integrable structure of Ginibre’s ensemble of real random matrices and a Pfaffian integration theorem *J. Stat. Phys.* **129** 1159–231
- [16] Forrester P J and Nagao T 2007 Eigenvalue statistics of the real Ginibre ensemble *Phys. Rev. Lett.* **99** 050603
- [17] Forrester P J and Nagao T 2008 Skew orthogonal polynomials and the partly symmetric real Ginibre ensemble *J. Phys. A: Math. Theor.* **41** 375003
- [18] Borodin A and Sinclair C D 2009 The Ginibre ensemble of real random matrices and its scaling limits *Commun. Math. Phys.* **291** 177–224
- [19] Sommers H-J 2007 Symplectic structure of the real Ginibre ensemble *J. Phys. A: Math. Theor.* **40** F671–6
- [20] Sommers H-J and Wicczorek W 2008 General eigenvalue correlations for the real Ginibre ensemble *J. Phys. A: Math. Theor.* **41** 405003
- [21] Akemann G, Phillips M J and Sommers H-J 2010 The chiral Gaussian two-matrix ensemble of real asymmetric matrices *J. Phys. A: Math. Theor.* **43** 085211
- [22] Osborn J C 2004 Universal results from an alternate random-matrix model for QCD with a baryon chemical potential *Phys. Rev. Lett.* **93** 222001
- [23] Akemann G 2005 The complex Laguerre symplectic ensemble of non-Hermitian matrices *Nucl. Phys. B* **730** 253–99
- [24] Forrester P J and Mays A 2011 Pfaffian point process for the Gaussian real generalised eigenvalue problem *Probab. Theor. Relat. Fields* at press (doi:10.1007/s00440-011-0361-8)
- [25] Khoruzhenko B A, Sommers H-J and Życzkowski K 2010 Truncations of random orthogonal matrices *Phys. Rev. E* **82** 040106(R)
- [26] Fyodorov Y V and Sommers H-J 2003 Random matrices close to Hermitian or unitary: overview of methods and results *J. Phys. A: Math. Gen.* **36** 3303–47
- [27] Khoruzhenko B A and Sommers H-J 2011 Non-Hermitian ensembles *Oxford Handbook of Random Matrix Theory* ed G Akemann, J Baik and P Di Francesco (New York: Oxford University Press) p 376
- [28] Mehta M L 2004 *Random Matrices* 3rd edn (New York: Academic)
- [29] Girko V L 1985 Circular law *Theory Probab. Appl.* **29** 694–706
- [30] Bai Z D 1997 Circular law *Ann. Probab.* **25** 494–529
- [31] Götze F and Tikhomirov A 2010 The circular law for random matrices *Ann. Probab.* **38** 1444–91
- [32] Tao T and Vu V 2008 Random matrices: the circular law *Commun. Contemp. Math.* **10** 261–307
- [33] Feinberg J and Zee A 1997 Non-Gaussian non-Hermitian random matrix theory: phase transition and addition formalism *Nucl. Phys. B* **501** 643–69
- [34] Feinberg J, Scalettar R and Zee A 2001 Single ring theorem and the disk-annulus phase transition *J. Math. Phys.* **42** 5718–40
- [35] Guionnet A, Krishnapur M and Zeitouni O 2011 The single ring theorem *Ann. Math.* **174** 1189–217

- [36] Wei Y and Fyodorov Y V 2008 On the mean density of complex eigenvalues for an ensemble of random matrices with prescribed singular values *J. Phys. A: Math. Theor.* **41** 502001
- [37] Bogomolny E 2010 Asymptotic mean density of sub-unitary ensembles *J. Phys. A: Math. Theor.* **43** 335102
- [38] Forrester P J 2010 *Log-Gases and Random Matrices* (Princeton, NJ: Princeton University Press)
- [39] Burda Z, Janik R A and Waclaw B 2010 Spectrum of the product of independent random gaussian matrices *Phys. Rev. E* **81** 041132
- [40] Burda Z, Jarosz A, Livan G, Nowak M A and Swiech A 2010 Eigenvalues and singular values of products of rectangular Gaussian random matrices *Phys. Rev. E* **82** 061114
- [41] Jarosz A 2010 Addition of free unitary random matrices II arXiv:1010.5220v1 [math-ph]
- [42] Życzkowski K and Sommers H J 2001 Induced measures in the space of mixed quantum states *J. Phys. A: Math. Gen.* **34** 7111–25
- [43] Życzkowski K and Sommers H-J 2000 Truncations of random unitary matrices *J. Phys. A: Math. Gen.* **33** 2045–57
- [44] Forrester P J 2006 Quantum conductance problems and the Jacobi ensemble *J. Phys. A: Math. Gen.* **39** 6861–70
- [45] Fischmann J 2012 *PhD Thesis* Queen Mary University of London (in preparation)
- [46] Abramowitz M and Stegun I A (ed) 1972 *Handbook of Mathematical Functions with Formulas, Graphs, and Mathematical Tables* (New York: Dover)
- [47] Forrester P J and Honner G 1999 Exact statistical properties of the zeros of complex random polynomials *J. Phys. A: Math. Gen.* **32** 2961–81
- [48] Akemann G 2001 Microscopic correlations of non-Hermitian Dirac operators in three-dimensional QCD *Phys. Rev. D* **64** 114021
- [49] Akemann G, Phillips M J and Shifrin L 2009 Gap probabilities in non-Hermitian random matrix theory *J. Math. Phys.* **50** 063504
- [50] Wei Y and Khoruzhenko B A 2009 $O(n)$ colour–flavour transformations and characteristic polynomials of real random matrices arXiv:0901.0746v1 [math-ph]
- [51] Fyodorov Y V and Khoruzhenko B A 2007 Averages of spectral determinants and ‘single ring theorem’ of Feinberg and Zee *Acta Phys. Pol. B* **38** 4067–77
- [52] Akemann G, Kieburg M and Phillips M J 2010 Skew-orthogonal Laguerre polynomials for chiral real asymmetric random matrices *J. Phys. A: Math. Theor.* **43** 375207
- [53] Edelman A, Kostlan E and Shub M 1994 How many eigenvalues of a random matrix are real? *J. Am. Math. Soc.* **7** 247–67
- [54] Bengtsson I and Życzkowski K 2006 *Geometry of Quantum States* (Cambridge: Cambridge University Press)
- [55] Bruzda W, Cappellini V, Sommers H-J and Życzkowski K 2009 Random quantum operations *Phys. Lett. A* **373** 320–4
- [56] Roga W, Smaczyński M and Życzkowski K 2011 Composition of quantum operations and products of random matrices *Acta Phys. Pol. B* **42** 1123–40
- [57] Holevo A S 2006 Complementary channels and the additivity problem *Theory Probab. Appl.* **51** 92–100
- [58] King C, Matsumoto K, Nathanson M and Ruskai M B 2007 Properties of conjugate channels with applications to additivity and multiplicativity *Markov Process. Relat. Fields* **13** 391–423
- [59] Guionnet A and Zeitouni O 2010 Support convergence in the single ring theorem arXiv:1012.2624